Received: 15 March 2022 | Revised: 20 June 2022 | Accepted: 22 June 2022

DOI: 10.1002/jnr.25103

RESEARCH ARTICLE

JOURNAL OF Neuroscience Research

Sex differences in morphine sensitivity are associated with differential glial expression in the brainstem of rats with neuropathic pain

Damien C. Boorman | **Kevin A. Keay**

School of Medical Sciences and the Brain and Mind Centre, The University of Sydney, Camperdown, New South Wales, Australia

Correspondence
Kevin A. Keay, School of Medical Sciences and the Brain and Mind Centre, The University of Sydney, 100 Mallet Street, Camperdown, NSW 2050, Australia.
Email: kevin.keay@sydney.edu.au

Funding information
NWG Macintosh Memorial Fund

Abstract

Chronic pain is more prevalent and reported to be more severe in women. Opioid analgesics are less effective in women and result in stronger nauseant effects. The neurobiological mechanisms underlying these sex differences have yet to be clearly defined, though recent research has suggested neuronal–glial interactions are likely involved. We have previously shown that similar to people, morphine is less effective at reducing pain behaviors in female rats. In this study, we used the immunohistochemical detection of glial fibrillary acidic protein (GFAP) expression to investigate sex differences in astrocyte density and morphology in six medullary regions known to be modulated by pain and/or opioids. Morphine administration had small sex-dependent effects on overall GFAP expression, but not on astrocyte morphology, in the rostral ventromedial medulla, the subnucleus reticularis dorsalis, and the area postrema. Significant sex differences in the density and morphology of GFAP immunopositive astrocytes were detected in all six regions. In general, GFAP-positive cells in females showed smaller volumes and reduced complexity than those observed in males. Furthermore, females showed lower overall GFAP expression in all regions except for the area postrema, the critical medullary region responsible for opioid-induced nausea and emesis. These data support the possibility that differences in astrocyte activity might underlie the sex differences seen in the processing of opioids in the context of chronic neuropathic pain.

KEYWORDS
astrocytes, emesis, GFAP, immunohistochemistry, medulla, opioids, RRID:AB_2313581, RRID:AB_477010

Abbreviations: ANOVA, analysis of variance; AP, area postrema; ARC, Animal Resource Centre; AUC, area under the curve; CCI, chronic constriction injury; cNTS, commissural nuclei of the solitary tract; DAB, 3–3′-diaminobenzidine tetrahydrochloride; EtOH, ethanol; GFAP, glial fibrillary acidic protein; NHS, normal horse serum; PBS, 0.1 M phosphate-buffered saline; PFA, paraformaldehyde; PGie, nucleus paragigantocellularis lateralis internus/externus; ROI, region of interest; RRID, research resource identifier; RVM, rostral ventromedial medulla; SpC, spinal cord; SRD, subnucleus reticularis dorsalis; TLR4, toll-like receptor 4; WA, Western Australia.

Edited by Cristina Antonella Ghiani and Tuan Trang. Reviewed by Anne Z. Murphy.

1 | INTRODUCTION

Emerging evidence continues to implicate astrocytes as critical players in the pathogenesis of chronic neuropathic pain states. Studies using preclinical animal models of neuropathic pain have consistently demonstrated changes in expression of astrocytic markers, such as glial fibrillary acidic protein (GFAP), at all levels of the neuraxis, during the development and maintenance of the pain state. Specifically, GFAP upregulation in response to a range of *neuropathic* injury models has been shown in the spinal cord (Colburn et al., 1997; Romero-Sandoval et al., 2008—male Sprague–Dawley rats), the brainstem (periaqueductal gray) (Mor et al., 2010—male Sprague–Dawley rats), the thalamus (Blaszczyk et al., 2018—male Wistar rats), and the amygdala (Marcello et al., 2013—male Sprague–Dawley rats), as well as cortical regions including the anterior cingulate cortex (Masocha, 2015—female BALB/c mice) and the somatosensory cortex (Kim et al., 2016—male C57BL/6 mice), see Tang et al. (2021) for review.

We have recently developed an animal model of opioid-conditioned placebo analgesia in female and male rats with chronic neuropathic pain (Boorman & Keay, 2021a, 2021b). In this protocol, rats received a unilateral chronic constriction injury of the sciatic nerve, and then, morphine-induced analgesia (6 mg/kg) was repeatedly paired with a range of multimodal contextual cues once per day over 4 days. On the fifth day, to elicit placebo analgesia, the rats were exposed to the contextual cues but administered saline instead of morphine, and their thermal pain sensitivity was compared to three control groups: a *natural history control* group, which received saline throughout the experiment; a *morphine control* group, which received morphine throughout the experiment; and an *acute morphine control* group, which received saline during conditioning but morphine on the fifth day. Using this experimental design, we found that: (i) 25% of females and 36% of males demonstrated strong placebo analgesic responses, (ii) morphine had reduced analgesic efficacy in females, and (iii) rats developed tolerance to the analgesic effects of morphine, an effect which appeared to be greatest in males. Importantly, each of these three findings mirrors observations of studies in human populations: (i) 30%–50% of people are strong placebo responders (Beecher, 1955; Kaptchuk et al., 2008; Tetreault et al., 2016); (ii) women require higher doses of opioids to achieve the same level of analgesia as men (Aubrun et al., 2005; Cepeda & Carr, 2003; Dahan et al., 2008); and (iii) men tend to escalate their opioid dosage more rapidly (Kaplovitch et al., 2015) and show higher levels of opioid addiction than women (Lee & Ho, 2013).

Underlying these disparities between the sexes are differences in the anatomy and activity of the descending pain modulatory system, the most well-characterized pathway being the periaqueductal gray (PAG) → rostral ventromedial medulla (RVM) → spinal cord (SpC). This pathway is activated during most analgesic responses, including analgesia produced endogenously (e.g., stress-induced analgesia (Butler & Finn, 2009)) and analgesia produced by exogenous opioids (e.g., systemic morphine administration (Averitt et al., 2019)).

Significance

This study investigates the expression of astrocytes in brainstem regions involved in the modulation of pain and the processing of opioids in female and male rats with neuropathic injury. These data implicate differences in astrocyte activity as a contributing factor in the commonly observed sex differences in the analgesic and emetic effects of opioids seen in both clinical and preclinical studies. We report sexually dimorphic glial activity in this context, highlighting a potential mechanism for these effects, and contribute to the reversal of the preclinical bias toward males when considering glial influences on the modulation of pain.

Studies have demonstrated that while female rats have a much larger PAG→RVM projection (twice the size), persistent pain and opioids activate the PAG→RVM projection more selectively in males (Loyd et al., 2007, 2008).

This PAG→RVM→SpC descending pathway also provides an effector mechanism by which higher order brain regions, such as the anterior cingulate cortex, medial prefrontal cortex, and amygdala, can powerfully modulate nociception. It is these higher order structures which presumably integrate contextual information with prior experience to initiate conditioned analgesia via descending pain modulation. Indeed, placebo analgesic responses are generally thought to be mediated through these same circuits in an opioid dependent manner (Crawford et al., 2021; Schafer et al., 2018). Several studies and reviews have recently suggested that glia (both astrocytes and microglia) play a significant role in the modulation of pain by influencing neuronal activity at the sites of the descending pain modulatory system (Averitt et al., 2019; Dubovy et al., 2018; Mo et al., 2022; Roberts et al., 2009; Sun et al., 2005; Tang et al., 2021). However, the precise ways in which opioids and chronic pain interact with astrocytes at the key sites of the descending pain modulatory pathway to influence analgesia are only just beginning to be understood. For example, it has recently been suggested that tolerance to the analgesic effects of morphine is due, at least partly, to adaptations in astrocytes in the vlPAG (see figure 2 in Averitt et al., 2019).

Our preclinical model of opioid conditioned analgesia presents a unique opportunity to investigate potential glial contributions to not just placebo analgesia, but also morphine-induced analgesia and tolerance, and importantly to identify sex differences in glial activity that might underlie our observed sex differences in morphine efficacy and tolerance (Boorman & Keay, 2021b). Therefore, in this study, we evaluated changes in astrocyte morphology, visualized using GFAP immunoreactivity, in six key medullary regions involved in pain transmission, pain modulation, and morphine sensitivity. These regions were the RVM (Chen & Heinricher, 2019; Fields et al., 1995), the subnucleus reticularis dorsalis (SRD) (Martins & Tavares, 2017), the paragigantocellularis lateralis internus/externus (PGie) (Zhu &

Zhou, 2010), the gracile nuclei (Boorman & Keay, 2021b), the commissural nuclei of the solitary tract (cNTS) (Boorman & Keay, 2021b), and the area postrema (Yoshikawa & Yoshida, 2002).

2 | METHODS

2.1 | Experimental design

This study investigated GFAP-expression in key sensory nuclei and pain modulatory regions in the medulla of both female and male rats that had a persistent peripheral neuropathic injury (sciatic nerve CCI). These rats had undergone a pharmacological conditioning procedure, whereby contextual cues were paired with the administration of morphine or saline, which elicited conditioned placebo analgesic responses. Strong placebo analgesia was demonstrated by 25% of females and 36% of males, who showed a ≥ 50% decrease in pain behaviors on a cold plate when exposed to the contextual cues when morphine was substituted for saline. These rats were classified as "placebo responders," while the remaining rats were classified as "non-responders." Three control groups were used: (i) a natural history control, which received saline during conditioning and again on Test Day (saline/saline), (ii) a morphine control group which received morphine during conditioning and again on Test Day (morphine/morphine), and (iii) an acute morphine group, which received saline during conditioning and morphine on Test Day (saline/morphine) (Figure 1).

Comparisons of medullary GFAP expression between these groups were made to investigate three questions. (1) Does acute or repeated morphine administration affect astrocyte morphology in the pain sensitive and pain modulatory regions of the brainstem medulla in rats with neuropathic pain? (2) Are there differences in astrocyte morphology in these regions between rats who demonstrated placebo analgesia (placebo responders) versus those that did not (nonreresponders)? (3) Finally, are there any sex differences in each of these groups? Coronal sections of the medulla from these rats were immunohistochemically labeled for glial fibrillary acidic protein (GFAP), an astrocyte-specific marker, and the density and morphology of the GFAP-immunoreactive astrocytes were quantified (Figure 2). The brain regions and nuclei analyzed included the rostral ventromedial medulla (RVM, which includes the raphe magnus), the subnucleus reticularis dorsalis (SRD), paragigantocellularis internal/external parts (PGie), the commissural nuclei of the solitary tract (cNTS), the dorsal column gracile nuclei, and the area postrema (Figure 3). All data are available to others upon request (please email the corresponding author).

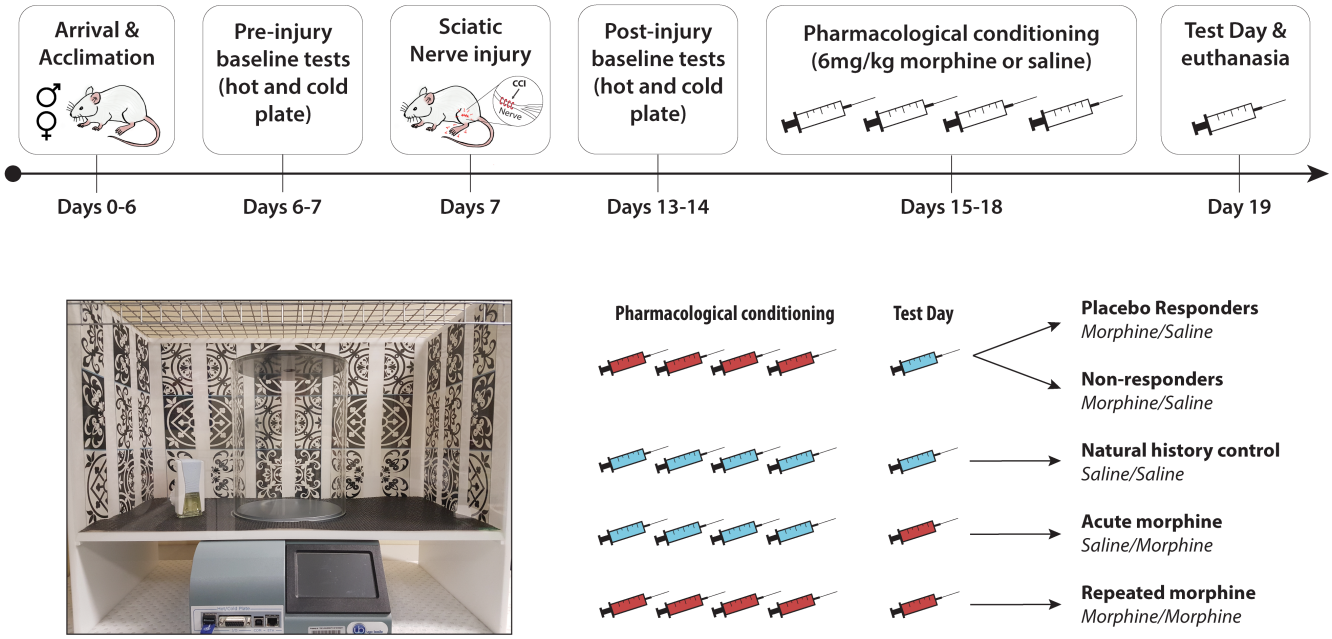

FIGURE 1 Experimental design. Six-week-old female ($n = 64$) and male ($n = 40$) rats were used for these experiments. After acclimation to laboratory conditions and pre-injury baseline thermal sensitivity testing (46°C hot plate and 5°C cold plate, Ugo Basile), all rats received a chronic constriction injury (CCI) of the right sciatic nerve. Six days later, rats underwent post-CCI baseline thermal sensitivity testing to ensure the development of allodynia. Rats that did not show at least five injured hind paw withdrawals over the 60 s thermal sensitivity tests were excluded from analysis. Over the next 4 days, rats underwent pharmacological conditioning, in which they received daily injections of either morphine (6 mg/kg, i.p) or volume-matched isotonic saline, and placed into a conditioning chamber (shown), where they again received thermal sensitivity testing. On the following day (Test Day), rats received either morphine or saline injections resulting in the experimental groups outlined above. Rats that received morphine during conditioning and saline on Test Day were classified as placebo responders if they demonstrated ≥50% reduction in hind paw withdrawals relative to their post-CCI baseline tests; otherwise, they were classified as nonresponders. Elements in this figure have been adapted from Figure 1 in Boorman and Keay (2021a).

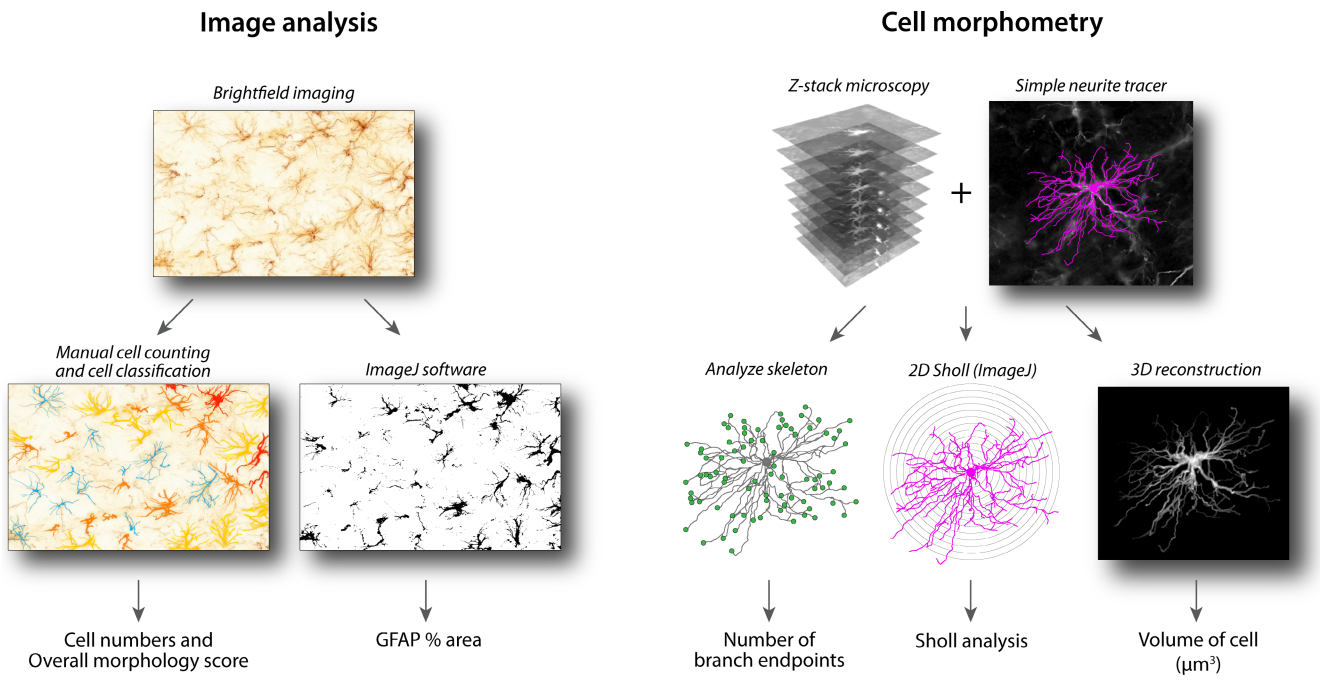

FIGURE 2 Image analysis and morphometric analysis of GFAP-immunopositive astrocytes. Images of each region of interest (ROI) were captured using bright-field microscopy at either 100× or 400× magnification. To determine the density of astrocytes in the regions of the RVM, SRD, and PGie, the numbers of GFAP immunoreactive cells per image were manually counted using the cell counter plugin within ImageJ. To determine overall GFAP expression in each ROI, the percentage area of GFAP labeling within each image was calculated in ImageJ. To determine the overall morphology score of the GFAP-positive astrocytes, each cell was manually classified using a modified version of the semiquantitative visual scale first described by Colburn et al. (1997), see Figure 4 for more details. To evaluate cell morphology, 3D reconstructions of GFAP-positive cells were created from Z-stacks (1000× magnification) using the simple neurite tracer toolbox within ImageJ and the number of branch endpoints and cell volume was calculated from these reconstructions. Additionally, to characterize the overall complexity of each cell, sholl profiles were calculated for each cell from 2D projections of these 3D reconstructions (see main text for more details).

2.2 | Animals and housing

All procedures in this study were approved by the University of Sydney Animal Care and Ethics committee (Project Number 1165). Procedures were designed and developed following the guidelines of the NHMRC "Code for Care and Use of Animals in Research in Australia" and the NSW Animal Research Act (2007). All efforts were made to employ the three R's (replacement, reduction, refinement) so as to minimize pain and discomfort where possible, and therefore also adhered to the IASP's "Ethical Guidelines for the Investigations of Experimental Pain in Conscious Animals".

Six-week-old female ($n = 64$) and male ($n = 40$) Sprague–Dawley rats (ARC, Perth, WA, Australia), weighing 170–220 g upon arrival were used for these experiments. Females and males were tested in separate cohorts, with all males tested first (2 months), then all females tested afterwards (3 months). At no time did males and females share housing or testing rooms. Rats were group housed, four per cage, in standard open-top polycarbonate cages and had ad libitum access to food (standard chow) and water. Both the housing room and testing room were temperature (22 ± 1°C) and humidity (40%–70%) controlled, with the housing room on a reversed 12:12 h light–dark cycle (lights OFF at 08:00) so as to align behavioral testing to when the rats are most active.

2.3 | Chronic constriction injury (CCI) surgery

All rats used in this study received a unilateral CCI of the sciatic nerve as first described by Bennett and Xie (1988). Female rats weighed between 200 and 240 g, while male rats weighed between 240 and 280 g at the time of surgery. To begin this procedure, rats were anesthetized using isoflurane (5% induction, 2.5% maintenance) in 100% O_2 (flow rate 1.5 L/min). Once the surgical plane of anesthesia was reached, the right hind limb was shaved and wiped with povidone-iodine, and a 2-cm incision was made alongside the femur. Gentle, blunt dissection through the biceps femoris allowed for the isolation of the sciatic nerve. Four ligatures (catgut chrome 5–0, Johnson & Johnson) were loosely tied around the nerve, immediately proximal to its trifurcation, spaced 1 mm apart, ensuring that the ligatures visibly compressed the nerve without occluding the epineural blood flow. The nerve was returned to its original position between the muscles and the incision closed with Michel clips. Several drops of lignocaine (20 mg/ml) were applied to the closed incision, and the entire region was dusted with topical antibiotic powder (Tricin®, Jurox). Finally, a mixture of petroleum jelly and quinine was applied to deter licking of the wound. After surgery, each rat was allowed to recover in an individual, open-top cage until ambulatory and alert (~30 min), before being returned to its home cage.

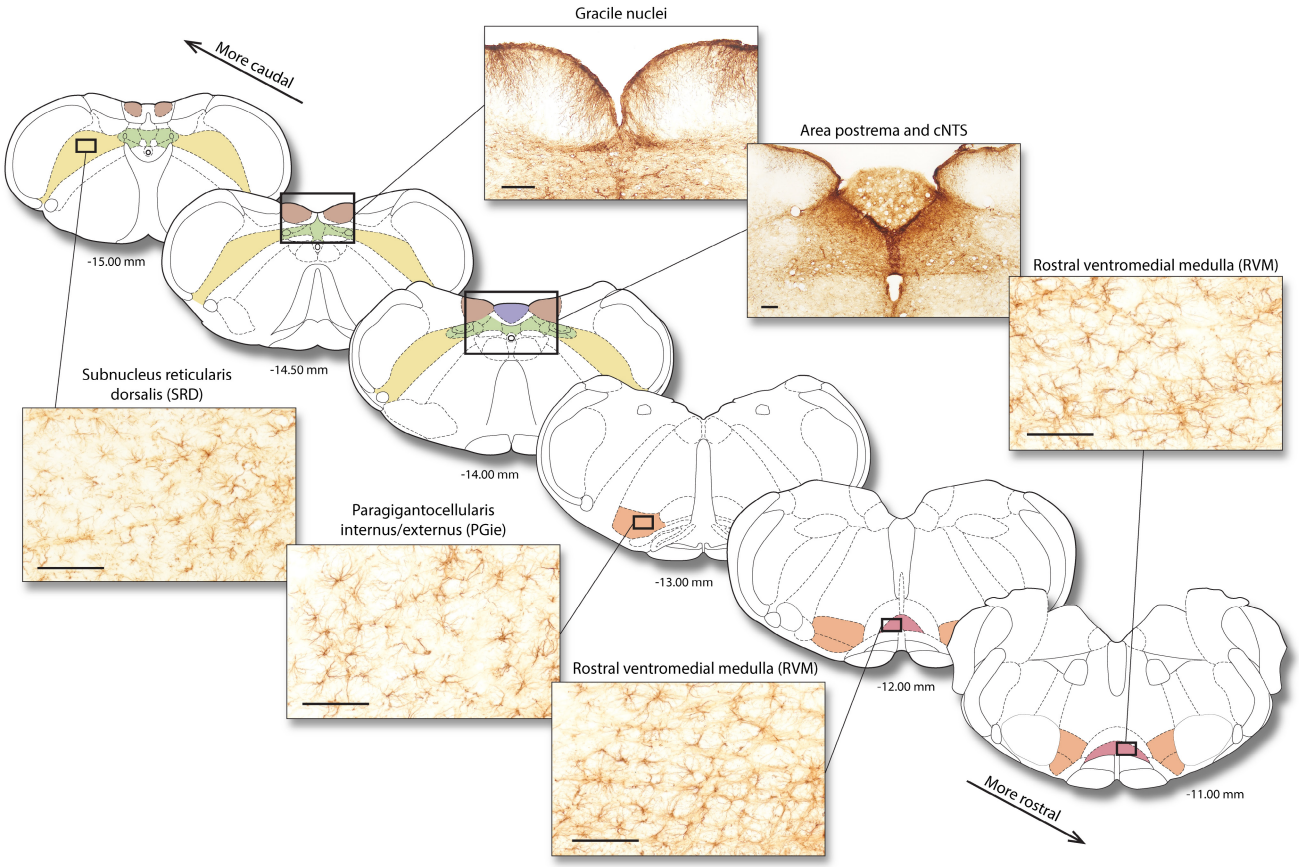

FIGURE 3 Regions of interest (ROIs) investigated in the medulla. 40 μm coronal sections were immunohistochemically labeled for glial fibrillary acidic protein (GFAP, RRID:AB_477010), and astrocyte density and morphology were assessed in each ROI (see Figure 2 for more details). ROIs were delineated using cytoarchitectural features of the tissue and with reference to the rat brain atlas of Paxinos and Watson (2005). The regions analyzed were the subnucleus reticularis dorsalis (SRD; yellow), gracile nuclei (brown), area postrema (purple), commissural nuclei of the solitary tract (cNTS, green), paragigantocellularis lateralis internus/externus (PGie; orange), and rostral ventromedial medulla (RVM; red). Example photomicrographs of GFAP staining are shown for each ROI. Scale bars represent 100 μm in all images. The distance from bregma is shown under each section.

2.4 | Pharmacological conditioning and behavioral testing

The pharmacological conditioning and behavioral testing procedures of these experiments have been described previously in detail (see Boorman & Keay, 2021b). Six days after CCI surgery, rats underwent post-CCI baseline thermal sensitivity testing using a hot/cold plate analgesiometer (Ugo Basile, Italy) to ensure the development of allodynia. Rats were first placed on the hot plate (60 s, plate set to 46°C), and then 15 min later the cold plate (60 s, plate set to 5°C). The number, latency, and cumulative duration of hind paw withdrawals were scored from video recordings. Rats that did not demonstrate sufficient allodynia at this post-CCI baseline (at least five hind paw withdrawals in 60 s) were excluded (n = 13 females and 5 males, see table 1 in Boorman & Keay, 2021b for further details).

To elicit conditioned placebo analgesia, morphine-induced analgesia was repeatedly paired with collection of multimodal contextual cues inside a custom-built conditioning chamber (see Figure 1), and the following day the rats were returned to this chamber but administered saline instead of morphine. To begin this procedure, rats received an intraperitoneal injection while in their housing room and were immediately transferred into the conditioning chamber, which was located in a separate testing room. The testing room was dimly lit to provide the visual context cue. Rats were left alone for 30 min before being tested on a hot plate (60 s, plate set to 46°C), and then 15 min later on a cold plate (60 s, plate set to 5°C). This thermal sensitivity testing was performed within the conditioning chamber in the presence of the contextual cues. Rats were returned to their home cage immediately following the cold plate test. This procedure was repeated once per day for five consecutive days.

Rats were assigned randomly to either receive the placebo treatment drug regimen or a drug treatment control regimen. Rats in the placebo treatment (n = 24F/14M) received morphine (6 mg/kg) for the first 4 days, and then saline on day 5 (i.e., Test Day). Three drug treatment control groups were used: (i) a natural history control, which received saline for all 5 days (saline/saline, n = 11F/8M), (ii) a morphine control group which received morphine for all 5 days (morphine/morphine, n = 9F/7M), and (iii) an acute morphine group, which received saline during the first four conditioning days and morphine on day 5 Test Day (saline/

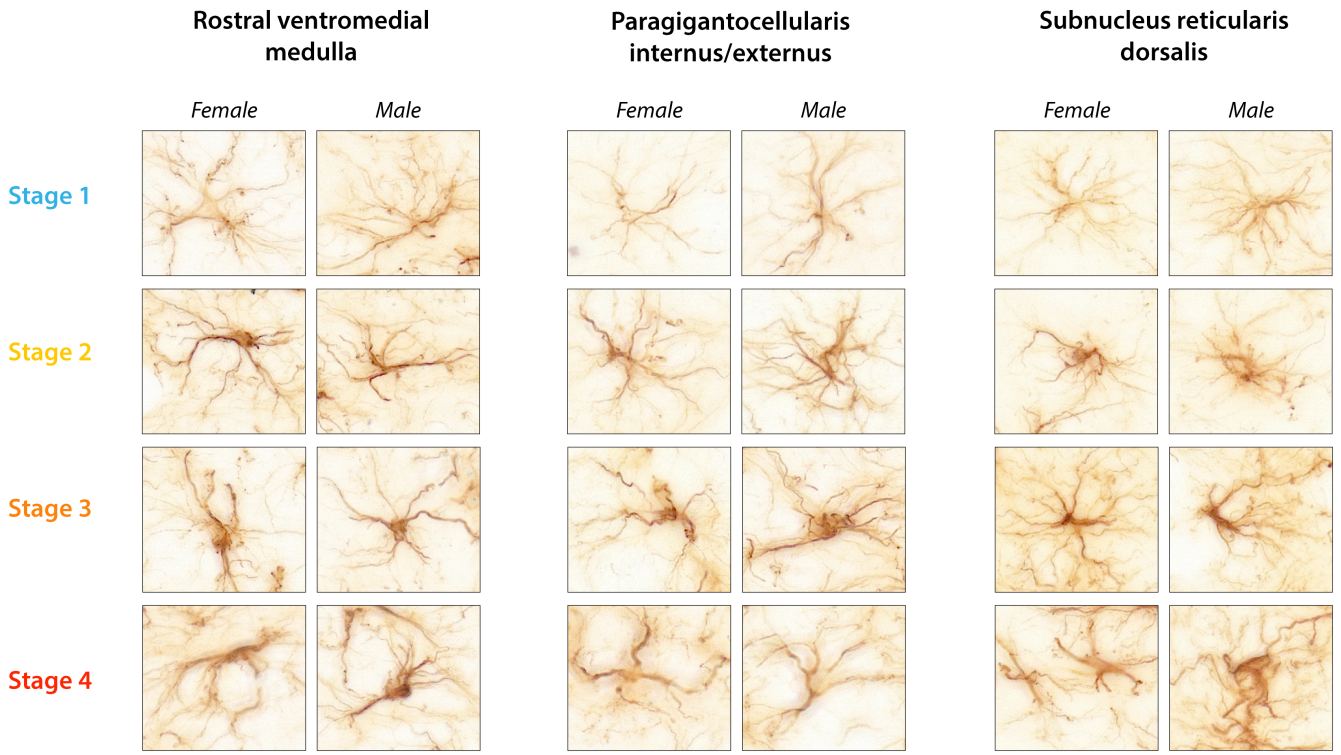

FIGURE 4 Overall morphology score of GFAP-positive astrocytes. The overall morphology score of all identifiable cells within each image taken of the rostral ventromedial medulla (RVM), paragigantocellularis lateralis internus/externus (PGie), and subnucleus reticularis dorsalis (SRD) were manually classified using a modified version of the semiquantitative visual scale described by Colburn et al. (1997). Each cell was scored as either at stage 1, 2, 3, or 4. A score of "1" indicated an astrocyte had extensive, fine, well-ramified projections, with a small soma. A score of "2" indicated an astrocyte was still well ramified but with thicker processes and/or a larger soma. A score of "3" indicated an astrocyte was less ramified, exhibiting stronger GFAP immunoreactivity with fewer processes and thicker soma. A score of "4" indicated an astrocyte had few processes, most of which were thick and bold, exhibiting strong immunoreactivity and a large, more rounded soma.

morphine, n = 7F/6M). Rats in the placebo treatment group were then classified as placebo responders or nonresponders based on their hind paw withdrawal behavior on Test Day. If a rat demonstrated a 50% or greater reduction in the number of paw withdrawals on Test Day compared to their own post-CCI baseline on either the hot plate or the cold plate, they were classified as a placebo responder; otherwise, they were classified as a nonresponder. As such, five of the 14 males and six of the 24 females that were in the placebo treatment group were classified as placebo responders. All behavioral data and analyses have been reported previously (see Boorman & Keay 2021b).

2.4.1 | Drug preparation and administration

All drug solutions were freshly prepared prior to injection. Morphine sulfate (DBL™, Hospira, USA) was diluted in 0.9% sterile saline to a concentration of 3 mg/ml and given as an intraperitoneal injection (6 mg/kg). Saline injections were prepared (volume matched) and administered in the same manner as the morphine injections.

2.5 | Perfusion and extraction

Two hours after the final conditioning procedure on Test Day, rats were euthanized with sodium pentobarbitone (130 mg/kg i.p) and transcardially perfused with 400 ml of heparinized 0.9% saline (4°C), followed by 400 ml of 4% paraformaldehyde in sodium acetate-borate buffer (pH 9.6, 4°C). Brains were immediately extracted and post-fixed in the same fixative for 30–60 min, before being transferred into 10% sucrose/0.1 M phosphate-buffered saline for storage at 4°C.

2.6 | Immunohistochemistry

The brains of 32 females and 28 males were chosen to undergo immunohistochemistry (Saline/Saline n = 7F/6M, Saline/Morphine n = 6F/5M, Morphine/Morphine n = 7F/6M, No Placebo n = 6F/6M, and Placebo n = 6F/5M). The brains from all placebo responders were used, with equal or greater numbers of brains arbitrarily selected from each of the remaining experimental groups for each sex. A brainstem block containing the medulla was isolated (approximately −8 to −16 mm from bregma) and cut into 40 µm coronal sections

using a cryostat (LEICA CM1950, Germany), which were collected in a 1:5 series and stored in antifreeze at −20°C until processing (Chan et al., 1993). Two of these series underwent immunohistochemical labelling for tryptophan hydroxylase (TPH) and/or c-Fos, the results of which have been published (Boorman & Keay, 2021b). A third series underwent immunohistochemical staining for glial fibrillary acidic protein (GFAP). The GFAP antibody (RRID:AB_477010) was chosen as it has been previously validated and reported in the Journal of Comparative Neurology antibody database and has been widely published since. Throughout immunohistochemical processing all washes were with 0.1 M phosphate-buffered saline (PBS) unless otherwise stated. Washes, incubations, and reactions all took place at room temperature, within glass vials, and on an orbital shaker at 100 rpm unless otherwise stated. All immunohistochemical procedures were run in four independent batches using the same reagents. Each batch contained animals from each of the experimental groups and each of the sexes, to remove any procedural biases. The visualization DAB reaction for each brain lasted 10–11 min.

To begin, free floating sections were removed from anti-freeze and washed thoroughly (3 × 10 min). Sections were then washed in 50% ethanol for 30 min for cell permeabilization, and then in 3% H_2O_2 in 50% ethanol for 30 min to quench endogenous peroxidase activity. Sections were washed (3 × 10 min), then placed into a blocking solution of 10% normal horse serum (NHS) in 0.1 M PBS for 30 min to reduce nonspecific antibody binding. Sections were then incubated in mouse monoclonal anti-GFAP IgG (1:5000 in 2% NHS/PBS; Sigma-Aldrich, St. Louis, USA) overnight at 4°C. The next day sections were washed and then incubated in horse anti-mouse IgG (1:500 in 2% NHS/PBS; Vector Laboratories, Burlingame, USA, RRID:AB_2313581) for 2 h, washed again, and then incubated in ExtrAvidin Peroxidase (1:1000 in PBS; Sigma-Aldrich) for 2.5 h. The bound antibody complex was visualized using 3,3′-diaminobenzidine tetrahydrochloride as the chromogen and the glucose oxidase method, which produced a brown precipitate. The reaction took place on ice (10–11 min) and was stopped with 4 × 10-min PBS washes. Sections were mounted onto gelatinized glass slides and allowed to dry for 48 h, after which they were dehydrated in ascending ethanol, delipidated with histolene, and coverslipped with DPX (Sigma) mounting medium. The brain sections from five male rats (2 Sal/Sal, 1 Mor/Mor, 2 No Placebo) were not analyzed due to tissue processing issues and excluded from analysis.

2.7 | Image acquisition and analysis

The brain regions of interest (ROIs) analyzed were chosen *ex ante based* on their known involvement in the transmission of hind limb sensation (i.e., gracile nuclei), pain transmission and modulation (i.e., RVM, PGie, SRD), or their involvement in visceral sensation, autonomic function, and chemoreception (i.e., cNTS and area postrema). It was hypothesized that astrocyte density and morphology in these regions would be significantly affected by either morphine administration or placebo analgesia. All images for analysis were captured using a Gryphax Kapella camera (Jenoptik®, Jena, Germany). ROIs were identified using the cytoarchitectural features of the tissue and the stereotaxic rat atlas of Paxinos and Watson (2005) as a guide. Each microscope slide was recoded to blind the experimenter (DB) during both image capture and analysis.

2.7.1 | Gross image analysis (GFAP-ir cell density, overall morphology score, % area stained)

To assess the density of GFAP immunoreactive astrocytes, their overall morphology score, and the % area stained in the ROIs described above, bright-field images were captured using an Olympus BX-51 at 100× (gracile nuclei, cNTS, area postrema) or 400× (RVM, SRD, PGie) magnification. Images analyzed at 400× were composed of four stacked images through the *Z*-plane, which were flattened in ImageJ using the <*Z project*> function to resolve depth of tissue focusing. Background was subtracted from all images using ImageJ <*subtract background*> function. For the SRD, one image on each side was captured per brain for analysis (300 μm [w] × 200 μm [h]), the center of which corresponded to the stereotaxic coordinates −14.3 mm posterior from bregma, ±2 mm from midline, +1.5 mm superior to the interaural line (Paxinos & Watson, 2005). For the RVM, three images (300 μm [w] × 200 μm [h]) per side per brain were captured at −10.5, −11.25, and −12.0 mm from bregma. For the PGie, three images (300 μm [w] × 200 μm [h]) per side per brain were captured at −11.5, −12.0, and −12.5 mm from bregma. For the gracile nuclei, three images per side were captured at −14.0, −14.5, and −15.0 mm from bregma. For the cNTS, three midline images were taken at −13.5, −14.0, and −14.5 mm from bregma, the most rostral of which was also used for the area postrema analysis.

For the RVM, PGie, and SRD, individual cell profiles were easily distinguished, so the total numbers of GFAP-ir cells per image were manually counted using the <*cell counter*> plugin within ImageJ (v. 2.0.0-rc-69/1.52p). Additionally, the overall morphology score of each GFAP-ir cell within each image was calculated based on a modified version of the semiquantitative visual scale first described by Colburn et al. (1997). Each cell was given a score of 1, 2, 3, or 4. A score of "1" indicated an astrocyte had extensive, fine, well-ramified projections, with a small soma. A score of "2" indicated an astrocyte was still well ramified but with thicker processes and/or a larger soma. A score of "3" indicated an astrocyte was less ramified, exhibiting stronger GFAP immunoreactivity with fewer processes and thicker soma. A score of "4" indicated an astrocyte had few processes, most of which were thick and "bold," exhibiting strong immunoreactivity and a large, more rounded soma (see Figure 4 for examples). Finally, the percentage area of GFAP-ir staining (sometimes referred to as "integrated density") per image was calculated using ImageJ. The image was first converted to <*8-bit*> and then the <*threshold*> and <*analyze particles*> functions were used to measure the % area of the image that was GFAP immunopositively stained.

The density of staining of GFAP-positive astrocytes in the gracile nuclei, cNTS, and area postrema, particularly in association with the glial limitans and the parenchymal basal lamina, precluded reliable delineation

of individual cell profiles, and therefore, only the % area of staining was used to make comparisons (see example images in Figure 2). For these ROIs, the relevant nuclei were isolated from the images using ImageJ and % area of staining calculated from the isolated area.

2.7.2 | Astrocyte morphology

To assess and compare astrocyte morphology in the RVM and the SRD, two GFAP-ir cells per brain per ROI (one left and one right) underwent morphometric analysis. These cells were chosen based on the following criteria: (i) they did not significantly overlap with a neighboring cell, (ii) the entire soma was contained within the section, (iii) they had limited physical interactions with adjacent blood vessels, and (iv) they were the closest cells to the predefined coordinates for each ROI (see Figures 5 and 6 for examples). The coordinates for the RVM were −11 mm posterior from bregma, ±0.4 mm from midline, and −0.4 mm inferior from the interaural line. The coordinates for the SRD were −14.3 mm posterior from bregma, ±2 mm from midline, and +1.5 mm superior to the interaural line. For each astrocyte, automated confocal *Z*-stacks were taken using a BX-61 connected to an Olympus IX2-UCB, which was controlled using µManager software (Edelstein et al., 2010). Images were taken at 1000× magnification using an oil immersion objective. *Z*-stacks consisted of 1920 (w) × 1200 (h) pixel 2D images taken every 0.3 µm throughout the depth of the tissue (~60–70 images per stack).

Z-stacked images were preprocessed in ImageJ using the <*subtract background*> and <*invert*> function to enhance staining contrast before being imported into the Simple Neurite Tracer toolbox for cell tracing and reconstruction (Arshadi et al., 2021). Simple Neurite Tracer allows for supervised, semi-automatic (Hessian-based A-star search algorithm) tracing of cells and their processes, constructing three-dimensional path information from *Z*-stacks. These path reconstructions were then used to assess several morphometric features of the astrocytes, including number of branch endpoints, cell volume, and sholl profile (see Figure 2). To calculate cell volume, the <*Fill Out*> function was used with a manually specified distance threshold (0.14) used for the fill search. Upon reaching this threshold, a binary image stack was produced, and the <*voxel counter*> function was used to estimate the volume of each cell from this image stack in μm^3. Sholl analysis was conducted to gauge the overall complexity of astrocytes, which quantifies branching density as a function of radial distance from the soma. The <*sholl analysis*> function was used on a 2D projection of the traced paths, with 2 µm increments between radii. The number of path intersections at each concentric circle was plotted against the distance from the center of the soma to give the sholl profile of each astrocyte.

2.8 | Statistical analysis

Statistical tests were done in GraphPad Prism version 9.0.1 (GraphPad Prism Software, San Diego, California, USA), with $\alpha = 0.05$. We did not detect any significant lateralization effects for any measure in any ROIs so data from left and right were averaged. Similarly, for ROIs in which more than one image was analyzed across the rostral–caudal axis (RVM, PGie, cNTS), data were averaged to give a single data point for each animal, for each measure, for each ROI. To assess differences in sholl profiles, the area under the curve (AUC) was calculated for each animal using the trapezoid rule. The likelihood that the sampled datasets came from normally distributed populations was assessed using the Anderson–Darling test, which evaluated the data distributions for males and females for each dependent measure in each ROI. Statistically significant deviations from the normal distribution were not seen for any of these measures in any of the regions except for the % area of GFAP staining in the RVM, cNTS, and area postrema. To assess whether acute or repeated morphine administration had sex-dependent effects on GFAP expression, two-way ANOVAs (*experimental group* × *sex*) between the natural history control (saline/saline), acute morphine (saline/morphine), and repeated morphine (morphine/morphine) groups were performed for each of the five main measures taken, in each of the ROIs investigated. To assess group differences in GFAP expression between placebo responders and non-responders, separate two-way ANOVAs (*experiment group* × *sex*) were conducted between these groups for each measure in each ROI. If a significant main effect or interaction effect was detected, then post hoc pairwise comparisons (Šidák correction) were used to assess differences between sexes or between experimental groups. The effect size for each factor is represented by omega squared (ω^2), which is an estimate of how much of the variance in the dependent variable (as a proportion between 0 and 1) is accounted for by the independent variables (i.e., the fixed factors).

Additionally, for the overall morphology score, which was an ordinal scale, and for the three datasets in which statistically significant deviations from normal distributions were detected, the Permutation Test, which is a nonparametric test for two-way factorial designs, was used to assess the statistical significance of the main and interaction effects of, and between, the independent factors (i.e., sex and experimental group). Mann–Whitney *U* tests were used for post hoc comparisons between groups, with the two-stage false discovery rate (Benjamini, Krieger, and Yekutieli) procedure used to correct for multiple comparisons. These tests yielded results comparable to their parametric equivalent (two-way ANOVAs), and thus, we report the results of the two-way ANOVAs in the results; and the details of the parameters and results of the Permutation Tests in Table S1. All graphs were created in GraphPad Prism and then exported into Adobe Illustrator 2021 (v 25.2) to create figurework.

3 | RESULTS

3.1 | GFAP expression in key medullary descending pain modulatory regions

Outputs of the neurons in the subnucleus reticularis dorsalis (SRD) and in the rostral ventromedial medulla (RVM), encompassing the serotonergic raphe magnus, are critical in the modulation of incoming

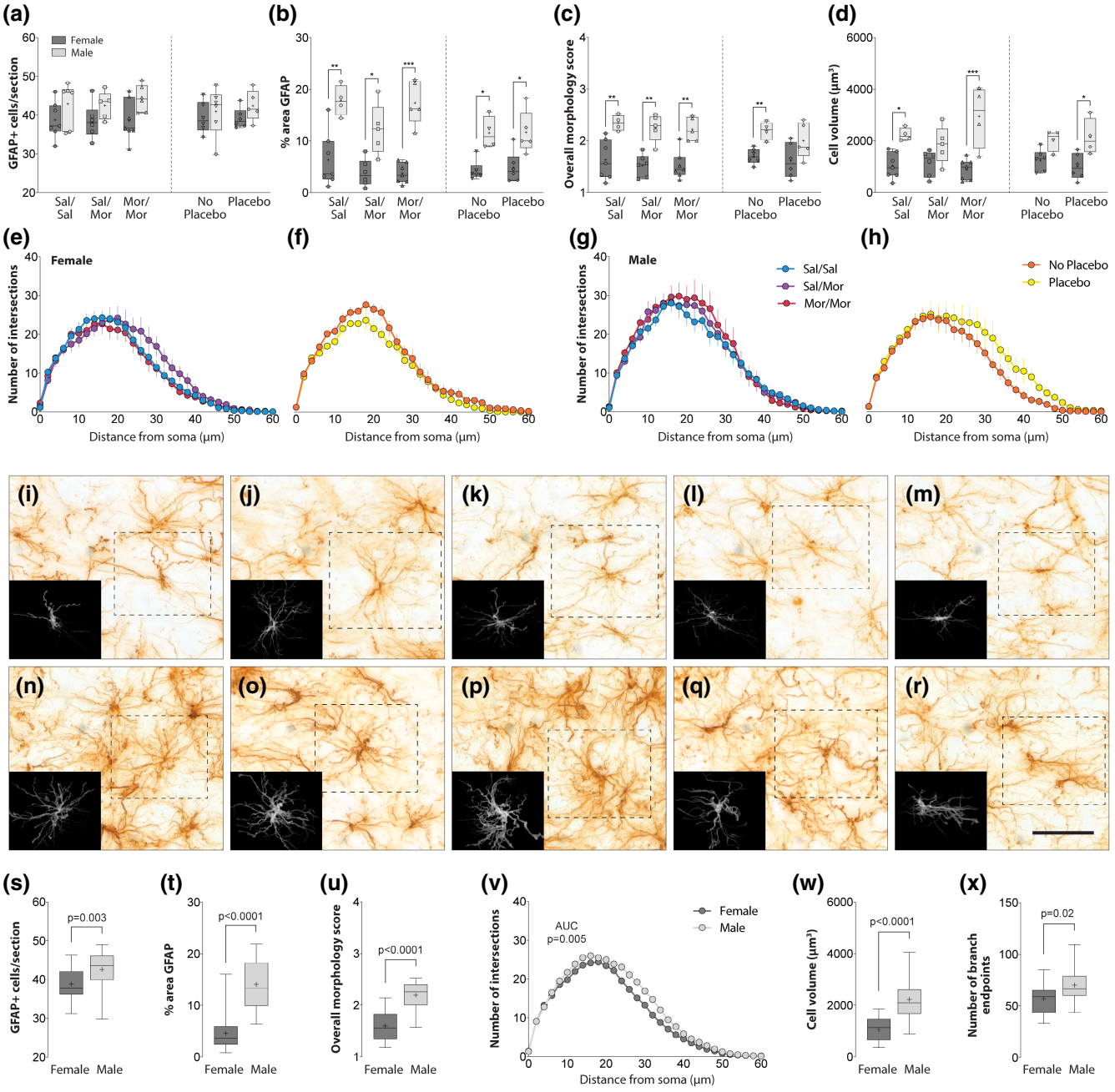

FIGURE 5 GFAP cell density, expression, and morphology in the rostral ventromedial medulla. (a–h) Comparisons between sex and drug treatment groups (natural history control [Sal/Sal, n = 7F/4M] vs. acute morphine [Sal/Mor, n = 6F/5M] vs. repeated morphine [Mor/Mor, n = 7F/5M]) or between sex and placebo responsiveness (no placebo [n = 6F,4M] vs. placebo [n = 6F/5M]) revealed that neither morphine administration nor placebo responsiveness had any effects on GFAP cell density (a), overall expression levels (b), overall morphology score (c), cell volume (d), or sholl profile (e–g). However, significant sex differences were detected among these groups. $^{*}p < .05$, $^{**}p < .001$, $^{***}p < .0001$, Sidak's pairwise comparisons, two-way ANOVAs. (i–r) Example photomicrographs of individual GFAP immunoreactive astrocytes isolated for morphometric analysis (dashed squares) from females (i–m) and males (n–r) in the natural history controls (i,n), acute morphine controls (j,o), repeated morphine controls (k,p), placebo nonresponders (l,q), and placebo responders (m,r). Insets depict renderings of 3D reconstructions used to quantify number of branch endpoints, cell volume, and sholl profiles. Scale bar represents 50 µm. Images were taken at 1000× magnification. (s–x) Box and whisker plots (min–max, line indicates median and + indicates mean values) showing underlying sex differences in GFAP cell density (s), overall GFAP expression (t), overall morphology score (u), sholl profile (v), cell volume (w), and the number of branch endpoints (x), p-values indicate main effects of sex from two-way ANOVAs or permutation tests (t,u).

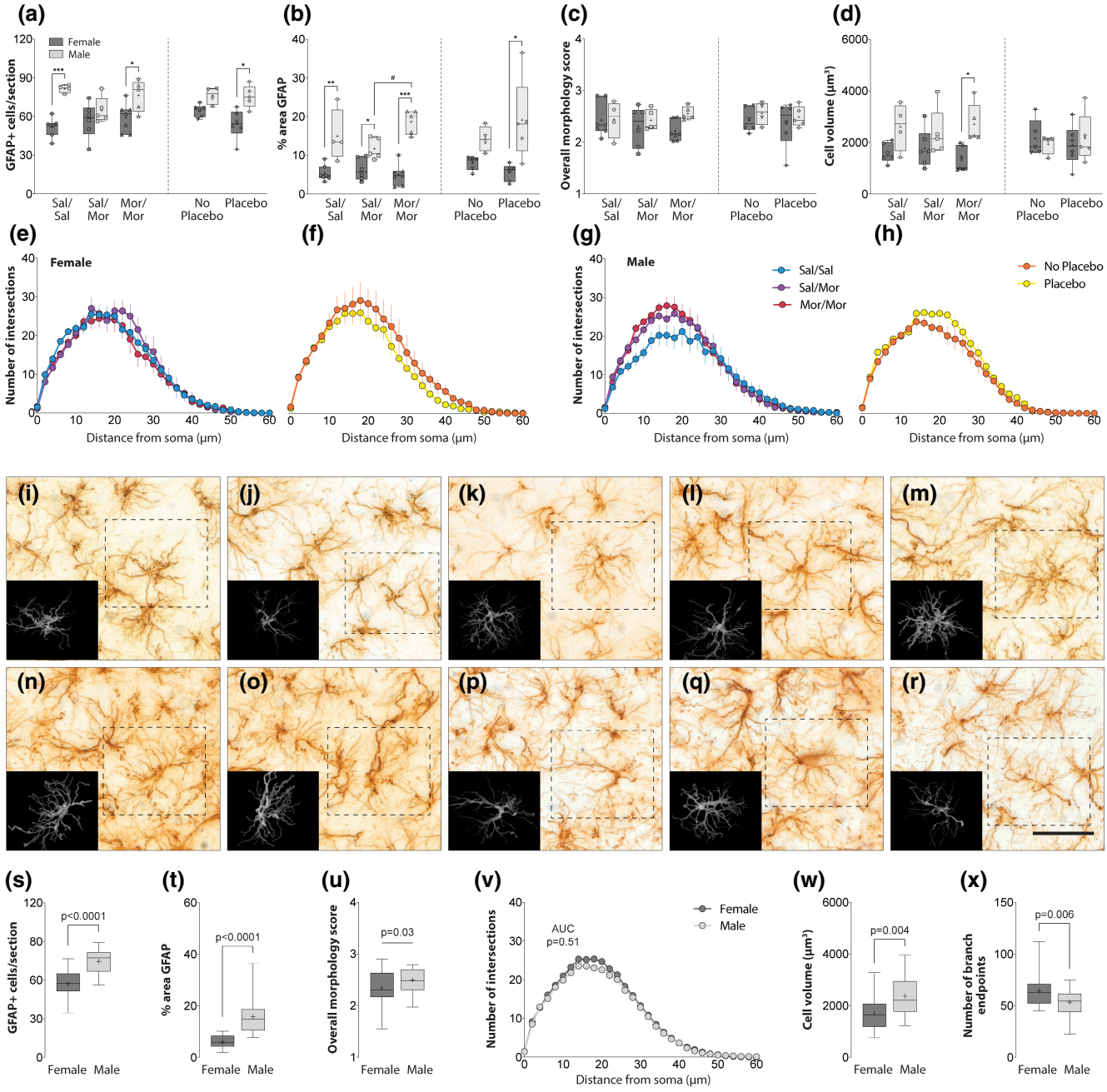

FIGURE 6 GFAP cell density, expression, and morphology in the subnucleus reticularis dorsalis. (a–h) Box and whisker plots (min to max) showing comparisons between sex and drug treatment groups (natural history control [Sal/Sal, n = 7F/4M] vs. acute morphine [Sal/Mor, n = 6F/5M] vs. repeated morphine [Mor/Mor, n = 7F/5M]), and between sex and placebo responsiveness (no placebo [n = 6F,4M] vs. placebo [n = 6F/5M]). $^{*}p < .05$, $^{**}p < .001$, $^{***}p < .0001$, Sidak's pairwise comparisons, $^{\#}p < .05$, Tukey's pairwise comparisons, two-way ANOVAs. (i–r) Example photomicrographs of individual GFAP immunoreactive astrocytes isolated for morphometric analysis (dashed squares) from females (i–m) and males (n–r) in the natural history controls (i,n), acute morphine controls (j,o), repeated morphine controls (k,p), placebo nonresponders (l,q), and placebo responders (m,r). Insets depict renderings of 3D reconstructions used to quantify the number of branch endpoints, cell volume, and sholl profiles. Scale bar represents 50 µm. Images were taken at 1000× magnification. (s–x) Box and whisker plots (min–max, line indicates median and + indicates mean values) showing comparisons between sexes in GFAP cell density (s), overall GFAP expression (t), overall morphology score (u), sholl profile (v), cell volume (w), and the number of branch endpoints (x), p-values indicate main effects of sex from two-way ANOVAs or permutation test (u).

nociceptive signals at the spinal and trigeminal levels. Their activity is regulated by exogenous opioids, both directly and indirectly. We detected large sex differences in the expression of GFAP in the natural history controls (saline/saline), acute morphine controls (saline/morphine), and repeated morphine controls (morphine/morphine).

3.1.1 | GFAP in the RVM (Figure 5)

GFAP-positive astrocytes were distributed remarkably uniformly between and around bundles of descending fibers throughout the raphe magnus in both male and female rats (see Figure 2). The average density of astrocytes for males in the RVM was ~710 cells/mm^2, while in females it was ~648 cells/mm^2. Neither single nor repeated administration of morphine had significant effects on the intensity of staining, the density of GFAP+ cells, or their morphology in either male or female rats. Additionally, we did not detect significant differences between placebo responders and nonresponders for any of the GFAP measures (see Table S1 for results of two-way ANOVAs). Comparisons between sexes revealed that males had approximately 10% more GFAP+ cells than females (42.6 ± 4.6 vs. 38.9 ± 4.1 cells/section, $p = .003$, $\omega^2 = 0.16$), and the processes of these cells were significantly thicker contributing to a greater percentage area of staining (14.1 ± 4.6% vs. 4.6 ± 3.2%, $p < .0001$, $\omega^2 = 0.61$) and larger cell volumes (2226 ± 165 μm^2 vs. 1057 ± 453 μm^2, $p = .003$, $\omega^2 = 0.50$). Males also had slightly more complex astrocyte profiles, as indicated by their greater Sholl AUC (771 ± 35 vs. 648 ± 25, $p = .005$, $\omega^2 = 0.14$), and greater numbers of branch endpoints (70 ± 15 vs. 57 ± 13, $p = .02$, $\omega^2 = 0.09$) (Figure 5s–x).

3.1.2 | GFAP in the subnucleus reticularis dorsalis (SRD; Figure 6)

GFAP-positive astrocytes were relatively evenly distributed throughout the SRD in both male and female rats (see Figure 2). The average density of astrocytes in the SRD was higher than in both the RVM and the PGie, with ~1242 cells/mm^2 in males, and ~951 cells/mm^2 in females. Rats that received acute morphine administration tended to have fewer numbers of GFAP+ astrocytes (and smaller percentage area of staining) than rats who received saline or morphine throughout the experiment. Neither acute nor repeated morphine administration affected the overall morphology score or cell volumes in either sex. Once again, we failed to detect significant differences between placebo responders and nonresponders for any of the GFAP measures (see Table S1 for results of two-way ANOVAs). Overall, males had approximately 25% more GFAP-positive astrocytes than females (74.5 ± 2.1 vs. 57.1 ± 1.8, $p < .0001$, $\omega^2 = 0.43$), resulting in greater GFAP percentage area stained (15.8 ± 1.3% vs. 5.9 ± 0.4%, $p < .0001$, $\omega^2 = 0.53$). Astrocytes in males had similar overall morphology scores to females (2.5 ± 0.04 vs. 2.3 ± 0.04, $p = .07$, $\omega^2 = 0.07$), with the cell volumes of males larger (2369 ± 167 μm^3 vs. 1717 ± 118 μm^3, $p = .004$, $\omega^2 = 0.15$) and somewhat less complex as indicated by fewer branch endpoints (53.4 ± 2.4 vs. 64.4 ± 2.9, $p = .006$, $\omega^2 = 0.13$). However, there was no sex difference in Sholl profile AUC (652 ± 29 vs. 679 ± 31, $p = .51$, $\omega^2 = 0.008$) (Figure 6s–x).

3.2 | GFAP expression in the nucleus paragigantocellularis lateralis internus/externus (PGie; Figure 7)

The PGie sits adjacent to the RVM and its cells may also contribute to descending modulatory influences on spinal cord nociceptive circuitry. GFAP-positive astrocytes showed a more heterogenous distribution in this region, which was most notable in its rostral extent adjacent to the facial nucleus (approximately −11 mm from bregma). Astrocyte density in this region was similar to that seen in the RVM, with 665 cells/mm^2 in males and 523 cells/mm^2 in females. Rats that received an acute dose of morphine had reduced percentage area of GFAP staining compared to both saline controls (saline/saline) and repeated morphine controls (morphine/morphine). Supporting this observation, a two-way ANOVA found a significant main effect of *experimental group* ($F_{2,28} = 5.176$, $p = .01$, $\omega^2 = 0.11$) and *sex* ($F_{1,28} = 59.15$, $p < .0001$, $\omega^2 = 0.60$), but no interaction between these factors ($F_{2,28} = 2.711$, $p = .08$, $\omega^2 = 0.06$). Acute morphine rats also tended to have fewer numbers of GFAP immunoreactive cells than these controls; however, a two-way ANOVA did not find significant effects of *experimental group* ($F_{2,28} = 2.220$, $p = .13$, $\omega^2 = 0.09$) or an interaction effect between *experimental group* and *sex* ($F_{2,28} = 1.618$, $p = .22$, $\omega^2 = 0.06$). Overall, males showed greater numbers of GFAP immunoreactive cells in the PGie (39.9 ± 1.3 vs. 31.4 ± 0.9, $p < .0001$, $\omega^2 = 0.39$), and a higher overall morphology score (2.1 ± 0.6 vs. 1.5 ± 0.4, $p < .0001$, $\omega^2 = 0.57$), both of which likely contributed to the greater percentage area of GFAP staining observed (14.3 ± 1.1 vs. 4.1 ± 0.4, $p < .0001$, $\omega^2 = 0.67$) (Figure 7n–p). While the effects of acute morphine administration seen in the PGie were not seen in the adjacent RVM, the sex differences appeared similar.

3.3 | GFAP expression in the somatosensory (gracile nucleus) and viscerosensory (cNTS) dorsal medullary nuclei (Figure 8a,b)

Astrocytes in the dorsomedial medulla were quite unlike those encountered in the SRD and the more rostral medullary regions described above. The density of staining of astrocytes, particularly in association with the glial limitans and the parenchymal basal lamina in this region, precluded reliable delineation of individual cell profiles; therefore, the thresholded area of staining of each image was used for comparisons. In the nucleus gracilis, labeled astrocytes were concentrated around the perimeter, the core of which contained a GFAP-negative region occupied by the ascending gracile funiculus fibers. We observed processes infiltrating the unstained core, presumably interdigitating with the axonal bundles (see Figure 3). Despite a unilateral CCI, there was no evidence for lateralized differences in GFAP staining. Furthermore, neither acute nor repeated morphine administration, or the presence of a placebo response was related to the expression of GFAP in the gracile nuclei. However, clear sex differences were observed in GFAP staining, with males showing significantly greater levels than females (21.6 ± 0.7% vs. 15.6 ± 0.5%, $p < .0001$, $\omega^2 = 0.48$).

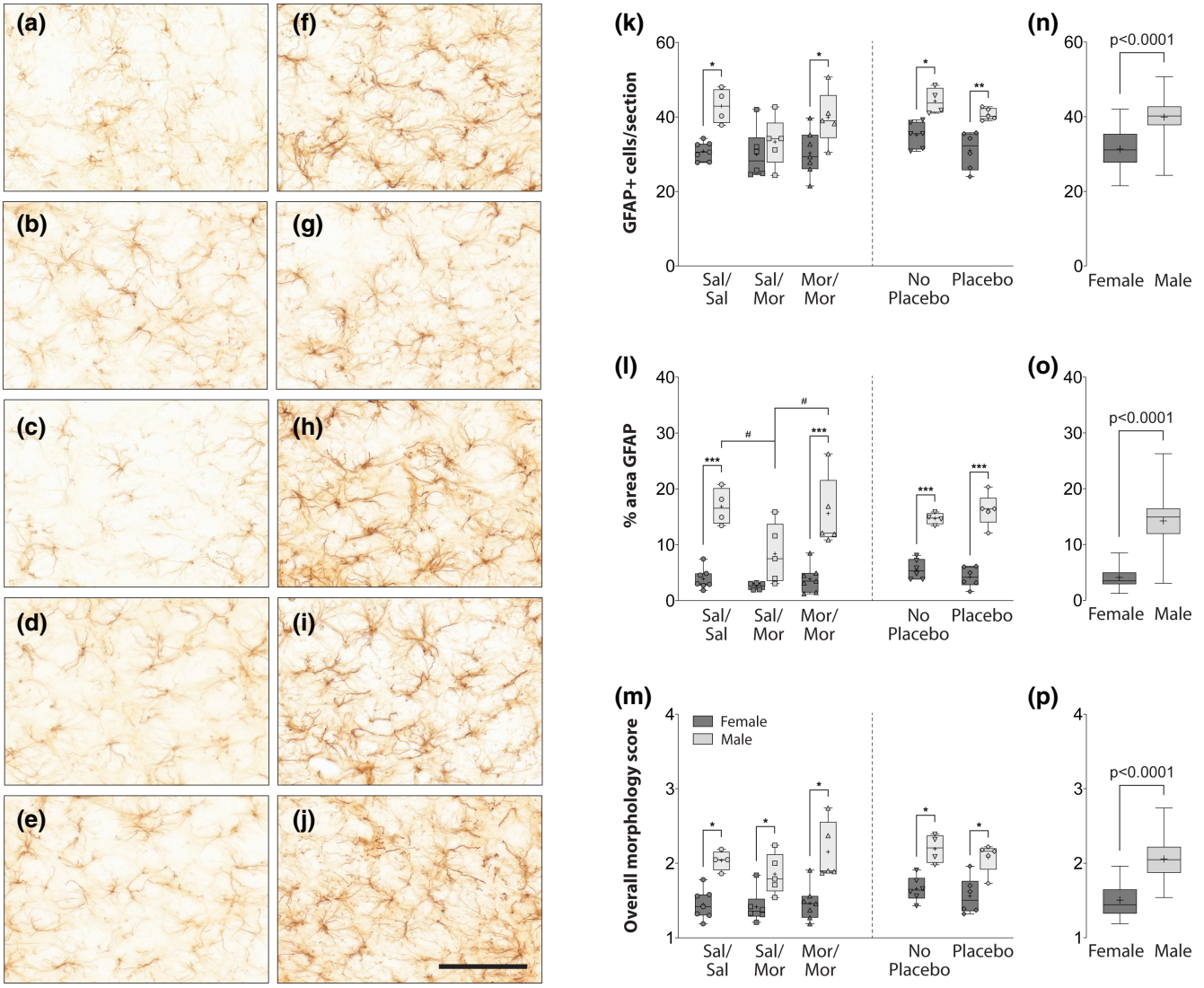

FIGURE 7 GFAP cell density, expression, and overall morphology score in the paragigantocellularis lateralis internus/externus (PGie). (a–j) Example photomicrographs of GFAP expression in the PGie taken at 400× magnification from females (a–e) and males (f–j) in the natural history controls (Sal/Sal; a,f), acute morphine controls (Sal/Mor; b,g), repeated morphine controls (Mor/Mor; c,h), placebo nonresponders (d,i), and placebo responders (e,j). Scale bar represents 100 μm. (k–m) box and whisker plots (min–max) showing comparisons between sex and drug treatment groups (natural history control [Sal/Sal, $n = 7F/4M$] vs. acute morphine [Sal/Mor, $n = 6F/5M$] vs. repeated morphine [Mor/Mor, $n = 7F/5M$]), and sex and placebo responsiveness (no placebo [$n = 6F,4M$] vs. placebo [$n = 6F/5M$]). $^{*}p < .05$, $^{**}p < .001$, $^{***}p < .0001$, Sidak's pairwise comparisons, $^{\#}p < .05$, Tukey's pairwise comparisons, two-way ANOVAs. (n–p) Boxplots (min–max, line indicates median and + indicates mean values) showing sex differences in GFAP cell density (n), overall GFAP expression (o), and overall morphology score (p), *p*-values indicate main effects of sex from two-way ANOVAs or permutation test (p).

In the commissural region of the nucleus of the solitary tract (cNTS), GFAP staining showed a distinctive pattern. It was most intense along its dorsal border (glial limitans/parenchymal basal lamina), abutting the area postrema, in a distinctive midline seam extending down to the central canal, becoming continuous with the ependymal cells of this structure. In the more ventral and lateral areas of the cNTS, the staining became progressively less dense, though nevertheless still challenging to resolve at the individual cellular level. Similar to our analysis of the nucleus gracilis, the staining was bilaterally symmetrical, and neither morphine administration nor the expression of placebo responses was related to GFAP expression (see Table S1 for statistical results). Clear sex differences were observed and, once again, pooled comparisons revealed that males showed significantly greater levels of GFAP than females ($32.6 \pm 6.4\%$ vs. $24.2 \pm 5.1\%$, $p < .0001$, $\omega^2 = 0.33$).

3.4 | GFAP expression in the area postrema (Figure 8c)

The chemosensitive area postrema is a circumventricular organ, whose activity in regulated by substances in systemic circulation

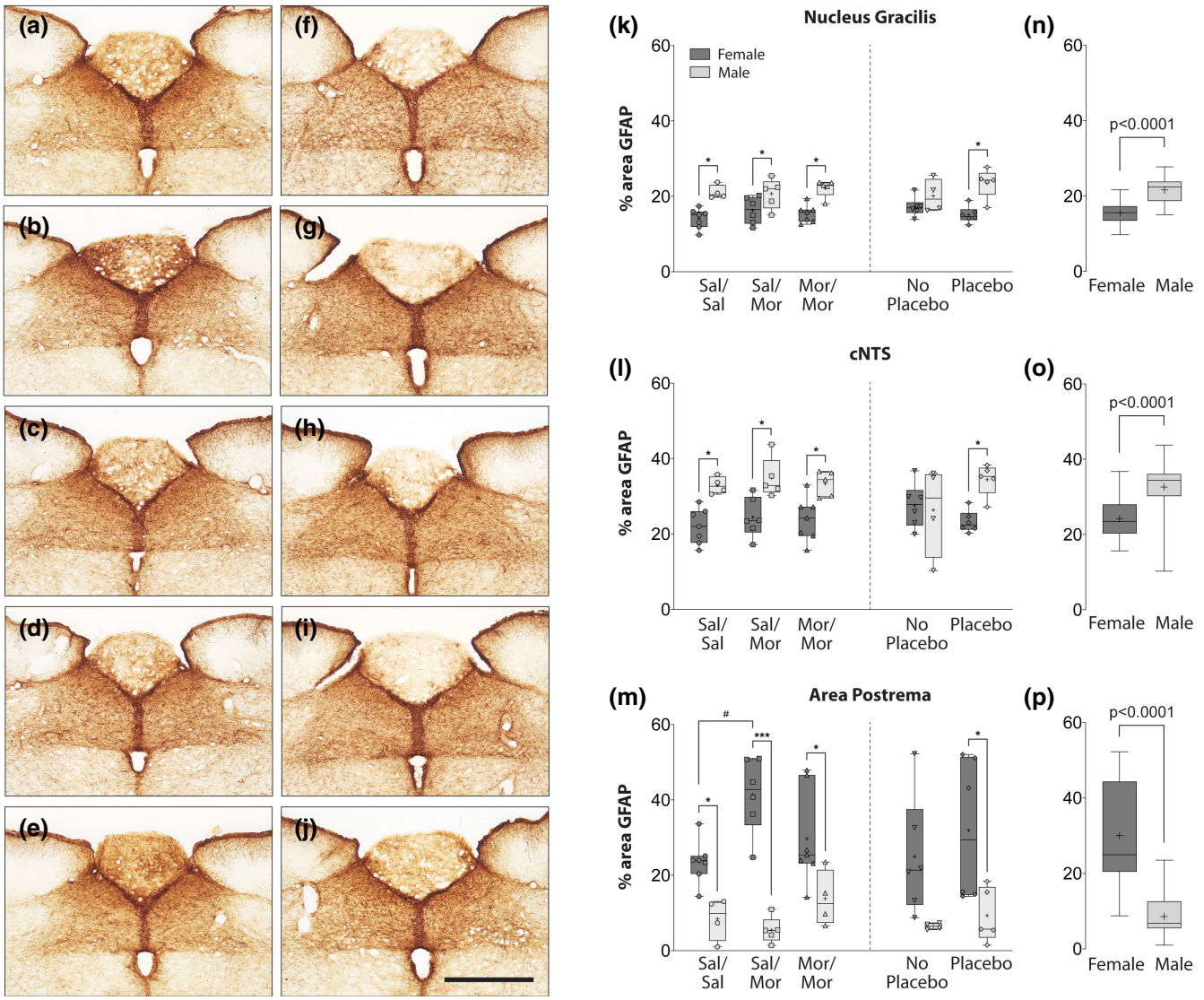

FIGURE 8 GFAP expression in the gracile nuclei, commissural nuclei of the solitary tract (cNTS), and area postrema. (a–j) Example photomicrographs of GFAP expression in these regions taken at 100× magnification from females (a–e) and males (f–j) in the natural history controls (Sal/Sal; a,f), acute morphine controls (Sal/Mor, b,g), repeated morphine controls (Mor/Mor, c,h), placebo nonresponders (d,i), and placebo responders (e,j). Scale bar represents 500 μm. (k–m) box and whisker plots (min–max) showing comparisons between sex and drug treatment groups (natural history control [Sal/Sal, n = 7F/4M] vs. acute morphine [Sal/Mor, n = 6F/5M] vs. repeated morphine [Mor/Mor, n = 7F/5M]), and sex and placebo responsiveness (no placebo [n = 6F,4M] vs. placebo [n = 6F/5M]). $^{*}p<.05$, $^{**}p<.001$, $^{***}p<.0001$, Sidak's pairwise comparisons, $^{\#}p<.05$, Tukey's pairwise comparisons, two-way ANOVAs. (n–p) Boxplots (min–max, line indicates median and + indicates mean values) showing sex differences in the percentage area of GFAP immunoreactive staining within the gracile nuclei (n), the cNTS (o), and the area postrema (p), p-values indicate main effects of sex from two-way ANOVAs or permutation test (o,p).

(Porreca & Ossipov, 2009). In stark contrast to the other areas we surveyed, GFAP staining was substantially greater in females compared to males (30.1 ± 2.4% vs. 8.6 ± 1.3). In the saline/saline controls, there was approximately double the area stained with GFAP in females compared to males. Two-way ANOVA found a significant effect of *sex* ($F_{1,28}$ = 53.47, $p<.0001$, ω^2 = 0.55), and an interaction effect between *sex* and *morphine* ($F_{2,28}$ = 5.084, p = .01, ω^2 = 0.11), with female rats who received acute morphine administration having significantly greater GFAP staining than the saline/saline controls (p = .003). Additionally, our data suggest that this increased GFAP activity in females diminishes with repeated morphine administration, with most rats in the morphine/morphine group showing similar levels as those seen in the saline/saline controls. Interestingly, male rats did not show these trends, with acute morphine-treated rats showing the least GFAP staining of the three groups. Once again, similar sex differences were detected for both the placebo responders and nonresponders ($F_{1,17}$ = 11.43, p = .004, ω^2 = 0.39), but no differences were found between these groups.

4 | DISCUSSION

The main questions driving this study were (i) to assess whether morphine altered the numbers and morphology of astrocytes in medullary regions known to be involved in pain transmission and modulation in rats with a neuropathic injury; (ii) to determine if there were any differences in the numbers and morphology of astrocytes in these regions between placebo responders and nonresponders; and (iii) to systematically evaluate sex differences in astrocyte numbers and morphology that became obvious when conducting analyses (i) and (ii). Astrocytes were evaluated by densitometric and morphometric analyses of GFAP expression. Unexpectedly, our data demonstrated that neither single dose nor repeated morphine administration (6 mg/kg) had significant effects on GFAP expression in the rostral ventromedial medulla (RVM). We did, however, detect sex-dependent effects of morphine administration on the % area of GFAP staining in the SRD, the PGie, and the area postrema, albeit with modest effect sizes. None of the other measures of GFAP expression (number of cells, overall morphology score, cell volume, sholl profile) were affected by morphine in these regions. Additionally, there were no differences in GFAP expression in any ROIs between placebo responders and nonresponders, suggesting that the susceptibility and expression of placebo analgesia are unrelated to brainstem glial activity.

The strongest finding from these results was large and consistent sex differences in the density and morphology of GFAP-positive astrocytes in nearly all regions investigated, regardless of experimental group. These sex differences were anatomically specific, with males generally showing higher numbers and/or greater GFAP expression in the RVM, SRD, PGie, gracile nuclei, and cNTS. In contrast, females displayed significantly greater GFAP expression in the area postrema.

These findings invite three important questions. Firstly, what are the likely implications of the observed sex differences in GFAP expression on pain modulation? Secondly, why did morphine have little or no effects on astrocyte numbers or morphology on the pain modulatory regions of the RVM, SRD, and PGie, and the opioid-responsive region of the cNTS? Finally, what are the likely implications of the observed sex differences in GFAP expression on opioid processing?

4.1 | Sex differences in GFAP expression

It is important to note that since all rats in this study received a CCI we are unable to directly resolve the effects of nerve constriction itself on GFAP expression. As such, there are two possible explanations for the significant and consistent sex differences in GFAP expression in the medullary regions we observed in this study. One possibility is that female and male rats have inherent, pre-existing differences in GFAP expression in these regions, likely reflecting sexually dimorphic glial activity. Underlying sex differences in astrocyte density, morphology, and GFAP expression has been reported in a number of CNS regions in the rat; these include the spinal cord (Posillico et al., 2015), hypothalamus (Kuo et al., 2010), hippocampus, and amygdala (Arias et al., 2009; Johnson et al., 2008) (see (Acaz-Fonseca et al., 2016) for review). In these regions, there is good evidence that sex steroids modulate astrocyte characteristics, even across the estrous cycle (Arias et al., 2009; Kuo et al., 2010). As far as we are aware, no previous studies have investigated underlying sex differences in GFAP expression in the medullary ROIs identified in this study. Our data suggest the possibility that such sex-steroid effects on astrocytes may be more generalized and include the lower brainstem, though direct comparisons between uninjured female and male controls are required to test this suggestion.

However, we also know that CCI and other models of chronic pain increase glial activity in the RVM (Mo et al., 2022; Roberts et al., 2009; Sun et al., 2005; Wei et al., 2008), the gracile nuclei (Gosselin et al., 2010), and the spinal cord (Chen et al., 2018; Colburn et al., 1997), as well as supramedullary regions including the PAG, but not in the anterior cingulate cortex or the nucleus accumbens (Michailidis et al., 2021). A second possibility, therefore, is that our observations reflect sex-dependent glial adaptations to the peripheral nerve injury, as have been described for the spinal cord (Vacca et al., 2014, 2021), a suggestion that has not previously been evaluated in our medullary ROIs. If this is the case, we think it is unlikely that the differences in glial GFAP expression and cell morphology can be attributed to sex differences in injury-evoked neuronal drive onto these regions, as we did not detect differences in c-Fos expression between males and females in the natural history controls in these same regions in our earlier study (see Boorman & Keay, 2021b).

4.2 | Morphine-induced minor changes in GFAP expression in the SRD and PGie

While we detected statistically significant differences in the % area of GFAP staining between saline controls, acute morphine, and repeated morphine in the SRD and PGie of males, there were no differences in either the numbers or morphology of these astrocytes. It is difficult, therefore, to determine the biological relevance of this observation. Other studies have previously reported large increases of GFAP expression following repeated morphine administration in the spinal cord, NTS, LC, VTA, hippocampus, and cingulate cortex (Alonso et al., 2007; Beitner-Johnson et al., 1993; Raghavendra et al., 2004; Song & Zhao, 2001). One possibility as to why we did not see equally large effects of repeated morphine administration is that it was administered on the background of a chronic neuropathic pain. Such an interaction has previously been reported for chronic inflammatory pain, whereby CFA administration prevented the GFAP increases in the vlPAG evoked by morphine (Eidson & Murphy, 2013). Finally, it is important to note that while we have focused on the effects of morphine administration on GFAP expression, the possibility that the differences in GFAP expression levels might in fact mediate the sex differences in morphine efficacy reported previously by us and many others cannot be discounted.

4.3 | Area postrema

Interestingly, the largest effect of morphine was found in the area postrema of females. Here, female rats, but not males, that were given acute morphine showed double the percentage area of GFAP compared to their saline-treated counterparts. Of the rats that received repeated morphine, on day five (Test Day), two of the seven continued to show increased GFAP expression, while the levels in the remaining five had returned to that of the saline controls. In contrast, morphine administration appeared to have negligible impacts on GFAP expression in the AP of male rats and furthermore, unlike the other medullary regions of interest investigated, male rats had less GFAP expression than females across all experimental groups.

Area postrema is a chemosensitive circumventricular organ, which detects levels of circulating chemicals and toxins. It is one of only three circumventricular organs that contains neurons and therefore can transduce these signals into neuronal activity. These neurons are neurochemically heterogenous, and include a significant GABAergic population of interneurons, whose activity regulates the excitatory drive of its output neurons. Potentially harmful levels of systemic toxins activate neurons within the AP, either directly or via inhibition of the GABAergic inhibitory interneurons (Guan et al., 1996). AP neurons project extensively to the caudal medulla and pons to trigger nausea, emesis, and behavioral aversion (Porreca & Ossipov, 2009). Ablation of the area postrema reliably abolishes the emetic responses to a range of drugs and compounds, including the opioids (Bhandari et al., 1992; Jovanovic-Micic et al., 1989; Strominger et al., 2001). In addition to these neuronal populations, the AP has resident glia, which include both astrocytes and microglia. Both neurons and glia are sensitive to systemic morphine, either via the presence of classical opioid receptors (μ- and ∂- subtypes) (Guan et al., 1997, 1999) or the immune-associated toll-like receptor 4 (TLR4) (Nakano et al., 2015; Watkins et al., 2009). Our data suggest that in female rats, morphine administration activates astrocytes either directly (via TLR4) and/or indirectly, via the disinhibition of the GABAergic population and subsequent increased activity of AP output neurons. Whereas in male rats, astrocytes in this region appear to be less sensitive to morphine, which may be due to decreased expression of TLR4 receptors.

Nausea and emesis are characteristic side effects of morphine administration in both animal models (i.e., ferrets) and humans, an effect that is both stronger and more prevalent in females (Apfel et al., 2012; Zun et al., 2002). That sex differences in glial activity and GFAP expression in the area postrema, such as we have observed in this study, might underlie the sex differences in the nauseant and emetic effects of opioids seen in people is a strong possibility.

4.4 | Summary

We have recently reported that in rats with a neuropathic injury, despite being able to detect injury-specific neuronal activation in the gracile nuclei, and morphine-specific neuronal activation in the cNTS, we were unable to detect differences between placebo responders and nonresponders in the pain modulatory regions of the medulla (Boorman & Keay, 2021b). We did not detect any sex differences in these regions, with the exception of a greater neuronal activation after morphine administration in the cNTS of males. Complementing this observation was the finding that morphine had significantly greater analgesic effects in males. In this study, we investigated whether placebo responders and nonresponders had differential glial GFAP expression or cell morphology in these same regions, which could influence the threshold and sensitivity of the circuitry that transmits and modifies pain. However, once again, we did not detect any differences in GFAP expression between placebo responders and nonresponders in any of the ROIs for either sex, suggesting that the expression of placebo is unrelated to glial activity in these regions.

Additionally, in comparing drug treatment control groups (i.e., saline/saline, saline/morphine, morphine/morphine), we found that morphine administration had minor impacts on GFAP expression in the SRD and PGie of male rats as well as moderate effects in the area postrema of females, with no apparent effects elsewhere. We also observed large and consistent sex differences in both the density and morphology of astrocytes in all ROIs investigated, irrespective of treatment group. In general, males had greater numbers of astrocytes, which tended to have greater volume, as well as greater overall GFAP expression (% area) in all regions except for the area postrema. In this particular region, female rats had significantly greater GFAP expression, which was further enhanced by acute morphine administration, and we have suggested these differences might underlie the clinical observations that females tend to experience greater nauseant and emetic effects from opioids. Finally, given that a major flaw in the preclinical pain literature has been a failure to address the effects of biological sex (Mogil, 2020), these data contribute to reversing the bias of a predominant focus of males when considering glial influences in the processing and modulation of pain after nerve injury.

AUTHOR CONTRIBUTIONS

Conceptualization, D.C.B., K.A.K.; *Methodology*, D.C.B., K.A.K.; *Software*, D.C.B.; *Validation*, D.C.B., K.A.K.; *Formal Analysis*, D.C.B.; *Investigation*, D.C.B.; *Data Curation*, D.C.B.; *Visualization*, D.C.B.; *Writing – Original Draft*, D.C.B., K.A.K.; *Writing – Review & Editing*, D.C.B, K.A.K.; *Resources*, K.A.K.; *Supervision*, K.A.K.; *Project Administration*, K.A.K.; *Funding Acquisition*, K.A.K.

ACKNOWLEDGMENTS

These experiments were supported by grants NWG Macintosh Memorial Fund, University of Sydney, Australia. We would like to thank and acknowledge Dr Jacques Raubenheimer for sharing his expertise and advice on elements of our statistical analyses. Open access publishing facilitated by The University of Sydney, as part of the Wiley - The University of Sydney agreement via the Council of Australian University Librarians.

CONFLICT OF INTEREST

The authors declare that they have no known competing financial interests or personal relationships that could have appeared to influence the work reported in this paper. The data that support the findings of this study are available from the corresponding author upon request.

DECLARATION OF TRANSPARENCY

The authors, reviewers and editors affirm that in accordance to the policies set by the *Journal of Neuroscience Research*, this manuscript presents an accurate and transparent account of the study being reported and that all critical details describing the methods and results are present.

PEER REVIEW

The peer review history for this article is available at https://publons.com/publon/10.1002/jnr.25103.

ORCID

Damien C. Boorman https://orcid.org/0000-0003-2819-1948
Kevin A. Keay https://orcid.org/0000-0003-3934-4380

REFERENCES

Acaz-Fonseca, E., Avila-Rodriguez, M., Garcia-Segura, L. M., & Barreto, G. E. (2016). Regulation of astroglia by gonadal steroid hormones under physiological and pathological conditions. *Progress in Neurobiology*, *144*, 5–26. https://doi.org/10.1016/j.pneurobio.2016.06.002

Alonso, E., Garrido, E., Díez-Fernández, C., Pérez-García, C., Herradón, G., Ezquerra, L., Deuel, T. F., & Alguacil, L. F. (2007). Yohimbine prevents morphine-induced changes of glial fibrillary acidic protein in brainstem and alpha2-adrenoceptor gene expression in hippocampus. *Neuroscience Letters*, *412*(2), 163–167. https://doi.org/10.1016/j.neulet.2006.11.002

Apfel, C. C., Heidrich, F. M., Jukar-Rao, S., Jalota, L., Hornuss, C., Whelan, R. P., Zhang, K., & Cakmakkaya, O. S. (2012). Evidence-based analysis of risk factors for postoperative nausea and vomiting. *British Journal of Anaesthesia*, *109*(5), 742–753. https://doi.org/10.1093/bja/aes276

Arias, C., Zepeda, A., Hernandez-Ortega, K., Leal-Galicia, P., Lojero, C., & Camacho-Arroyo, I. (2009). Sex and estrous cycle-dependent differences in glial fibrillary acidic protein immunoreactivity in the adult rat hippocampus. *Hormones and Behavior*, *55*(1), 257–263. https://doi.org/10.1016/j.yhbeh.2008.10.016

Arshadi, C., Gunther, U., Eddison, M., Harrington, K. I. S., & Ferreira, T. A. (2021). SNT: A unifying toolbox for quantification of neuronal anatomy. *Nature Methods*, *18*(4), 374–377. https://doi.org/10.1038/s41592-021-01105-7

Aubrun, F., Salvi, N., Coriat, P., & Riou, B. (2005). Sex- and age-related differences in morphine requirements for postoperative pain relief. *Anesthesiology*, *103*(1), 156–160. https://doi.org/10.1097/00000542-200507000-00023

Averitt, D. L., Eidson, L. N., Doyle, H. H., & Murphy, A. Z. (2019). Neuronal and glial factors contributing to sex differences in opioid modulation of pain. *Neuropsychopharmacology*, *44*(1), 155–165. https://doi.org/10.1038/s41386-018-0127-4

Beecher, H. K. (1955). The powerful placebo. *Journal of the American Medical Association*, *159*(17), 1602–1606. https://doi.org/10.1001/jama.1955.02960340022006

Beitner-Johnson, D., Guitart, X., & Nestler, E. J. (1993). Glial fibrillary acidic protein and the mesolimbic dopamine system: Regulation by chronic morphine and Lewis-Fischer strain differences in the rat ventral tegmental area. *Journal of Neurochemistry*, *61*(5), 1766–1773. https://doi.org/10.1111/j.1471-4159.1993.tb09814.x

Bennett, G. J., & Xie, Y. K. (1988). A peripheral mononeuropathy in rat that produces disorders of pain sensation like those seen in man. *Pain*, *33*(1), 87–107. https://doi.org/10.1016/0304-3959(88)90209-6

Bhandari, P., Bingham, S., & Andrews, P. L. (1992). The neuropharmacology of loperamide-induced emesis in the ferret: The role of the area postrema, vagus, opiate and 5-HT3 receptors. *Neuropharmacology*, *31*(8), 735–742. https://doi.org/10.1016/0028-3908(92)90034-m

Blaszczyk, L., Maitre, M., Leste-Lasserre, T., Clark, S., Cota, D., Oliet, S. H. R., & Fenelon, V. S. (2018). Sequential alteration of microglia and astrocytes in the rat thalamus following spinal nerve ligation. *Journal of Neuroinflammation*, *15*(1), 349. https://doi.org/10.1186/s12974-018-1378-z

Boorman, D. C., & Keay, K. A. (2021a). Escalating morphine dosage fails to elicit conditioned analgesia in a preclinical chronic neuropathic pain model. *Behavioural Pharmacology*, *32*(6), 479–486. https://doi.org/10.1097/FBP.0000000000000642

Boorman, D. C., & Keay, K. A. (2021b). Morphine-conditioned placebo analgesia in female and male rats with chronic neuropathic pain: C-Fos expression in the rostral ventromedial medulla. *Neuroscience*, *457*, 51–73. https://doi.org/10.1016/j.neuroscience.2020.11.038

Butler, R. K., & Finn, D. P. (2009). Stress-induced analgesia. *Progress in Neurobiology*, *88*(3), 184–202. https://doi.org/10.1016/j.pneurobio.2009.04.003

Cepeda, M. S., & Carr, D. B. (2003). Women experience more pain and require more morphine than men to achieve a similar degree of analgesia. *Anesthesia and Analgesia*, *97*(5), 1464–1468. https://doi.org/10.1213/01.ANE.0000080153.36643.83

Chan, R. K., Brown, E. R., Ericsson, A., Kovacs, K. J., & Sawchenko, P. E. (1993). A comparison of two immediate-early genes, c-fos and NGFI-B, as markers for functional activation in stress-related neuroendocrine circuitry. *Journal of Neuroscience*, *13*(12), 5126–5138.

Chen, G., Luo, X., Qadri, M. Y., Berta, T., & Ji, R. R. (2018). Sex-dependent glial signaling in pathological pain: Distinct roles of spinal microglia and astrocytes. *Neuroscience Bulletin*, *34*(1), 98–108. https://doi.org/10.1007/s12264-017-0145-y

Chen, Q., & Heinricher, M. M. (2019). Descending control mechanisms and chronic pain. *Current Rheumatology Reports*, *21*(5), 13. https://doi.org/10.1007/s11926-019-0813-1

Colburn, R. W., DeLeo, J. A., Rickman, A. J., Yeager, M. P., Kwon, P., & Hickey, W. F. (1997). Dissociation of microglial activation and neuropathic pain behaviors following peripheral nerve injury in the rat. *Journal of Neuroimmunology*, *79*(2), 163–175. https://doi.org/10.1016/s0165-5728(97)00119-7

Crawford, L. S., Mills, E. P., Hanson, T., Macey, P. M., Glarin, R., Macefield, V. G., Keay, K. A., & Henderson, L. A. (2021). Brainstem mechanisms of pain modulation: A within-subjects 7T fMRI study of placebo analgesic and nocebo hyperalgesic responses. *Journal of Neuroscience*, *41*(47), 9794–9806. https://doi.org/10.1523/JNEUROSCI.0806-21.2021

Dahan, A., Kest, B., Waxman, A. R., & Sarton, E. (2008). Sex-specific responses to opiates: Animal and human studies. *Anesthesia and Analgesia*, *107*(1), 83–95. https://doi.org/10.1213/ane.0b013e31816a66a4

Dubovy, P., Klusakova, I., Hradilova-Svizenska, I., Joukal, M., & Boadas-Vaello, P. (2018). Activation of astrocytes and microglial cells and CCL2/CCR2 upregulation in the dorsolateral and ventrolateral nuclei of periaqueductal gray and rostral ventromedial medulla following different types of sciatic nerve injury. *Frontiers in Cellular Neuroscience*, *12*, 40. https://doi.org/10.3389/fncel.2018.00040

Edelstein, A., Amodaj, N., Hoover, K., Vale, R., & Stuurman, N. (2010). Computer control of microscopes using microManager. *Current*

Protocols in Molecular Biology, Chapter 14, Unit 14 20. https://doi.org/10.1002/0471142727.mb1420s92

Eidson, L. N., & Murphy, A. Z. (2013). Persistent peripheral inflammation attenuates morphine-induced periaqueductal gray glial cell activation and analgesic tolerance in the male rat. *Journal of Pain*, *14*(4), 393–404. https://doi.org/10.1016/j.jpain.2012.12.010

Fields, H. L., Malick, A., & Burstein, R. (1995). Dorsal horn projection targets of ON and OFF cells in the rostral ventromedial medulla. *Journal of Neurophysiology*, *74*(4), 1742–1759. https://doi.org/10.1152/jn.1995.74.4.1742

Gosselin, R. D., Bebber, D., & Decosterd, I. (2010). Upregulation of the GABA transporter GAT-1 in the gracile nucleus in the spared nerve injury model of neuropathic pain. *Neuroscience Letters*, *480*(2), 132–137. https://doi.org/10.1016/j.neulet.2010.06.023

Guan, J. L., Wang, Q. P., & Nakai, Y. (1997). Electron microscopic observation of delta-opioid receptor-1 in the rat area postrema. *Peptides*, *18*(10), 1623–1628. https://doi.org/10.1016/s0196-9781(97)00234-9

Guan, J. L., Wang, Q. P., & Nakai, Y. (1999). Electron microscopic observation of mu-opioid receptor in the rat area postrema. *Peptides*, *20*(7), 873–880. https://doi.org/10.1016/s0196-9781(99)00075-3

Guan, J. L., Wang, Q. P., Shioda, S., Ochiai, H., & Nakai, Y. (1996). GABAergic synaptic innervation of catecholaminergic neurons in the area postrema of the rat. *Acta Anatomica*, *156*(1), 46–52. https://doi.org/10.1159/000147827

Johnson, R. T., Breedlove, S. M., & Jordan, C. L. (2008). Sex differences and laterality in astrocyte number and complexity in the adult rat medial amygdala. *Journal of Comparative Neurology*, *511*(5), 599–609. https://doi.org/10.1002/cne.21859

Jovanovic-Micic, D., Strbac, M., Krstic, S. K., Japundzic, N., Samardzic, R., & Beleslin, D. B. (1989). Ablation of the area postrema and emesis. *Metabolic Brain Disease*, *4*(1), 55–60. https://doi.org/10.1007/BF00999494

Kaplovitch, E., Gomes, T., Camacho, X., Dhalla, I. A., Mamdani, M. M., & Juurlink, D. N. (2015). Sex differences in dose escalation and overdose death during chronic opioid therapy: A population-based cohort study. *PLoS ONE*, *10*(8), e0134550. https://doi.org/10.1371/journal.pone.0134550

Kaptchuk, T. J., Kelley, J. M., Deykin, A., Wayne, P. M., Lasagna, L. C., Epstein, I. O., Kirsch, I., & Wechsler, M. E. (2008). Do "placebo responders" exist? *Contemporary Clinical Trials*, *29*(4), 587–595. https://doi.org/10.1016/j.cct.2008.02.002

Kim, S. K., Hayashi, H., Ishikawa, T., Shibata, K., Shigetomi, E., Shinozaki, Y., Inada, H., Roh, S. E., Kim, S. J., Lee, G., Bae, H., Moorhouse, A. J., Mikoshiba, K., Fukazawa, Y., Koizumi, S., & Nabekura, J. (2016). Cortical astrocytes rewire somatosensory cortical circuits for peripheral neuropathic pain. *Journal of Clinical Investigation*, *126*(5), 1983–1997. https://doi.org/10.1172/JCI82859

Kuo, J., Hamid, N., Bondar, G., Dewing, P., Clarkson, J., & Micevych, P. (2010). Sex differences in hypothalamic astrocyte response to estradiol stimulation. *Biology of Sex Differences*, *1*(1), 7. https://doi.org/10.1186/2042-6410-1-7

Lee, C. W., & Ho, I. K. (2013). Sex differences in opioid analgesia and addiction: Interactions among opioid receptors and estrogen receptors. *Molecular Pain*, *9*, 45. https://doi.org/10.1186/1744-8069-9-45

Loyd, D. R., Morgan, M. M., & Murphy, A. Z. (2007). Morphine preferentially activates the periaqueductal gray-rostral ventromedial medullary pathway in the male rat: A potential mechanism for sex differences in antinociception. *Neuroscience*, *147*(2), 456–468. https://doi.org/10.1016/j.neuroscience.2007.03.053

Loyd, D. R., Morgan, M. M., & Murphy, A. Z. (2008). Sexually dimorphic activation of the periaqueductal gray-rostral ventromedial medullary circuit during the development of tolerance to morphine in the rat. *European Journal of Neuroscience*, *27*(6), 1517–1524. https://doi.org/10.1111/j.1460-9568.2008.06100.x

Marcello, L., Cavaliere, C., Colangelo, A. M., Bianco, M. R., Cirillo, G., Alberghina, L., & Papa, M. (2013). Remodelling of supraspinal neuroglial network in neuropathic pain is featured by a reactive gliosis of the nociceptive amygdala. *European Journal of Pain*, *17*(6), 799–810. https://doi.org/10.1002/j.1532-2149.2012.00255.x

Martins, I., & Tavares, I. (2017). Reticular formation and pain: The past and the future. *Frontiers in Neuroanatomy*, *11*, 51. https://doi.org/10.3389/fnana.2017.00051

Masocha, W. (2015). Astrocyte activation in the anterior cingulate cortex and altered glutamatergic gene expression during paclitaxel-induced neuropathic pain in mice. *PeerJ*, *3*, e1350. https://doi.org/10.7717/peerj.1350

Michailidis, V., Lidhar, N. K., Cho, C., & Martin, L. J. (2021). Characterizing sex differences in depressive-like behavior and glial brain cell changes following peripheral nerve injury in mice. *Frontiers in Behavioral Neuroscience*, *15*, 758251. https://doi.org/10.3389/fnbeh.2021.758251

Mo, S. Y., Bai, S. S., Xu, X. X., Liu, Y., Fu, K. Y., Sessle, B. J., Cao, Y., & Xie, Q. F. (2022). Astrocytes in the rostral ventromedial medulla contribute to the maintenance of oro-facial hyperalgesia induced by late removal of dental occlusal interference. *Journal of Oral Rehabilitation*, *49*(2), 207–218. https://doi.org/10.1111/joor.13211

Mogil, J. S. (2020). Qualitative sex differences in pain processing: Emerging evidence of a biased literature. *Nature Reviews Neuroscience*, *21*(7), 353–365. https://doi.org/10.1038/s41583-020-0310-6

Mor, D., Bembrick, A. L., Austin, P. J., Wyllie, P. M., Creber, N. J., Denyer, G. S., & Keay, K. A. (2010). Anatomically specific patterns of glial activation in the periaqueductal gray of the sub-population of rats showing pain and disability following chronic constriction injury of the sciatic nerve. *Neuroscience*, *166*(4), 1167–1184. https://doi.org/10.1016/j.neuroscience.2010.01.045

Nakano, Y., Furube, E., Morita, S., Wanaka, A., Nakashima, T., & Miyata, S. (2015). Astrocytic TLR4 expression and LPS-induced nuclear translocation of STAT3 in the sensory circumventricular organs of adult mouse brain. *Journal of Neuroimmunology*, *278*, 144–158. https://doi.org/10.1016/j.jneuroim.2014.12.013

Paxinos, G., & Watson, C. (2005). *The rat brain in stereotaxic coordinates* (5th ed.). Elsevier Academic Press.

Porreca, F., & Ossipov, M. H. (2009). Nausea and vomiting side effects with opioid analgesics during treatment of chronic pain: Mechanisms, implications, and management options. *Pain Medicine*, *10*(4), 654–662. https://doi.org/10.1111/j.1526-4637.2009.00583.x

Posillico, C. K., Terasaki, L. S., Bilbo, S. D., & Schwarz, J. M. (2015). Examination of sex and minocycline treatment on acute morphine-induced analgesia and inflammatory gene expression along the pain pathway in Sprague-Dawley rats. *Biology of Sex Differences*, *6*, 33. https://doi.org/10.1186/s13293-015-0049-3

Raghavendra, V., Tanga, F. Y., & DeLeo, J. A. (2004). Attenuation of morphine tolerance, withdrawal-induced hyperalgesia, and associated spinal inflammatory immune responses by propentofylline in rats. *Neuropsychopharmacology*, *29*(2), 327–334. https://doi.org/10.1038/sj.npp.1300315

Roberts, J., Ossipov, M. H., & Porreca, F. (2009). Glial activation in the rostroventromedial medulla promotes descending facilitation to mediate inflammatory hypersensitivity. *European Journal of Neuroscience*, *30*(2), 229–241. https://doi.org/10.1111/j.1460-9568.2009.06813.x

Romero-Sandoval, A., Chai, N., Nutile-McMenemy, N., & Deleo, J. A. (2008). A comparison of spinal Iba1 and GFAP expression in rodent models of acute and chronic pain. *Brain Research*, *1219*, 116–126. https://doi.org/10.1016/j.brainres.2008.05.004

Schafer, S. M., Geuter, S., & Wager, T. D. (2018). Mechanisms of placebo analgesia: A dual-process model informed by insights from cross-species comparisons. *Progress in Neurobiology*, *160*, 101–122. https://doi.org/10.1016/j.pneurobio.2017.10.008

Song, P., & Zhao, Z. Q. (2001). The involvement of glial cells in the development of morphine tolerance. *Neuroscience Research*, *39*(3), 281–286. https://doi.org/10.1016/s0168-0102(00)00226-1

Strominger, N. L., Brady, R., Gullikson, G., & Carpenter, D. O. (2001). Imiquimod-elicited emesis is mediated by the area postrema, but not by direct neuronal activation. *Brain Research Bulletin*, *55*(3), 445–451. https://doi.org/10.1016/s0361-9230(01)00539-1

Sun, Y. N., Luo, J. Y., Rao, Z. R., Lan, L., & Duan, L. (2005). GFAP and Fos immunoreactivity in lumbo-sacral spinal cord and medulla oblongata after chronic colonic inflammation in rats. *World Journal of Gastroenterology*, *11*(31), 4827–4832. https://doi.org/10.3748/wjg.v11.i31.4827

Tang, J., Bair, M., & Descalzi, G. (2021). Reactive astrocytes: Critical players in the development of chronic pain. *Frontiers in Psychiatry*, *12*, 682056. https://doi.org/10.3389/fpsyt.2021.682056

Tetreault, P., Mansour, A., Vachon-Presseau, E., Schnitzer, T. J., Apkarian, A. V., & Baliki, M. N. (2016). Brain connectivity predicts placebo response across chronic pain clinical trials. *PLoS Biology*, *14*(10), e1002570. https://doi.org/10.1371/journal.pbio.1002570

Vacca, V., Marinelli, S., De Angelis, F., Angelini, D. F., Piras, E., Battistini, L., Pavone, F., & Coccurello, R. (2021). Sexually dimorphic immune and neuroimmune changes following peripheral nerve injury in mice: Novel insights for gender medicine. *International Journal of Molecular Sciences*, *22*(9), 4397. https://doi.org/10.3390/ijms22094397

Vacca, V., Marinelli, S., Pieroni, L., Urbani, A., Luvisetto, S., & Pavone, F. (2014). Higher pain perception and lack of recovery from neuropathic pain in females: A behavioural, immunohistochemical, and proteomic investigation on sex-related differences in mice. *Pain*, *155*(2), 388–402. https://doi.org/10.1016/j.pain.2013.10.027

Watkins, L. R., Hutchinson, M. R., Rice, K. C., & Maier, S. F. (2009). The "toll" of opioid-induced glial activation: Improving the clinical efficacy of opioids by targeting glia. *Trends in Pharmacological Sciences*, *30*(11), 581–591. https://doi.org/10.1016/j.tips.2009.08.002

Wei, F., Guo, W., Zou, S., Ren, K., & Dubner, R. (2008). Supraspinal glial-neuronal interactions contribute to descending pain facilitation. *Journal of Neuroscience*, *28*(42), 10482–10495. https://doi.org/10.1523/JNEUROSCI.3593-08.2008

Yoshikawa, T., & Yoshida, N. (2002). Effect of 6-hydroxydopamine treatment in the area postrema on morphine-induced emesis in ferrets. *Japanese Journal of Pharmacology*, *89*(4), 422–425. https://doi.org/10.1254/jjp.89.422

Zhu, H., & Zhou, W. (2010). Discharge activities of neurons in the nucleus paragigantocellularis during the development of morphine tolerance and dependence: A single unit study in chronically implanted rats. *European Journal of Pharmacology*, *636*(1–3), 65–72. https://doi.org/10.1016/j.ejphar.2010.03.033

Zun, L. S., Downey, L. V., Gossman, W., Rosenbaumdagger, J., & Sussman, G. (2002). Gender differences in narcotic-induced emesis in the ED. *American Journal of Emergency Medicine*, *20*(3), 151–154. https://doi.org/10.1053/ajem.2002.32631

SUPPORTING INFORMATION

Additional supporting information can be found online in the Supporting Information section at the end of this article.

TABLE S1 Results of two-way (*experimental group* × *sex*) ANOVAs for all measures and all ROIs investigated. Morphine comparisons involved the natural history control (saline/saline) versus acute morphine administration (saline/morphine) versus repeated morphine (morphine/morphine) groups. Placebo comparisons involved placebo responders versus nonresponders. The effect size for each factor is represented by omega squared (ω^2), which is an estimate of how much of the variance in the dependent variable (as a proportion between 0 and 1) is accounted for by the independent variables (i.e., the fixed factors). For the overall morphology score, which is an ordinal scale, and for the three datasets in which statistically significant deviations from normal distributions were detected (% area of GFAP staining in the RVM, cNTS, and area postrema), the Permutation test, which is a nonparametric test for two-way factorial designs, was used to assess the statistical significance of the main and interaction effects of and between the independent factors (i.e., sex vs. experimental groups). This analysis was performed in R version 3.6.1, using RStudio version 1.4.1106 and the *ez* package (Lawrence, 2016). For each test, 1000 permutations were computed. $^{*}p < .05$, $^{**}p < .001$, $^{***}p < .0001$. The results of these tests are placed alongside the results of standard two-way ANOVAs (as described above) for comparison. cNTS, commisural nuclei of the solitary tract; PGie, paragigantocellularis lateralis internus/externus; RVM, rostral ventromedial medulla, SRD, subnucleus reticularis dorsalis

Transparent Science Questionnaire for Authors

How to cite this article: Boorman, D. C., & Keay, K. A. (2022). Sex differences in morphine sensitivity are associated with differential glial expression in the brainstem of rats with neuropathic pain. *Journal of Neuroscience Research*, *100*, 1890–1907. https://doi.org/10.1002/jnr.25103